MATERIALS DEVELOPMENT FOR SOLAR CELL APPLICATIONS

FINAL REPORT

Period Covered:
1 June 1965 through 31 May 1966
Contract NAS5-9576

Prepared for:

NATIONAL AERONAUTICS AND SPACE ADMINISTRATION
Goddard Space Flight Center
Greenbelt, Maryland

FACILITY FORM 602

N66 37213 (ACCESSION NUMBER) (THRU)
78 (PAGES) 1 (CODE)
CR-78132 (NASA CR OR TMX OR AD NUMBER) 03 (CATEGORY)

GPO PRICE $
CFSTI PRICE(S) $
Hard copy (HC) 3.00
Microfiche (MF) .75
July 65

Prepared by:

Electronic Components and Devices
RADIO CORPORATION OF AMERICA
Industrial Tube and Semiconductor Division
Mountaintop, Pennsylvania

June 25, 1966

MATERIALS DEVELOPMENT FOR SOLAR CELL APPLICATIONS

FINAL REPORT

Period Covered:
1 June 1965 through 31 May 1966
Contract NAS5-9576

Prepared for:

NATIONAL AERONAUTICS AND SPACE ADMINISTRATION
Goddard Space Flight Center
Greenbelt, Maryland

Prepared by:

A. R. Topfer
Project Engineer

Approved by:

A. M. Splinter
Project Supervisor

Prepared by:

Electronic Components and Devices
RADIO CORPORATION OF AMERICA
Industrial Tube and Semiconductor Division
Mountaintop, Pennsylvania

June 25, 1966

FOREWORD

This is the Final Report for the twelve (12) month program, "Materials Development for Solar Cell Applications", Contract NAS5-9576, covering the period 1 June 1965 through 31 May 1966. This report has been prepared by the Advanced Development Laboratory, Direct Energy Conversion Department, Special Electronic Components Division, Radio Corporation of America, Mountaintop, Pennsylvania.

Principals in the research and development studies were Mr. Alvin R. Topfer, Project Engineer, and Mr. Walter J. Bartholomay.

The work was performed under the administration of Mr. M. Schach and Dr. P. H. Fang, Contract Technical Officer, Goddard Space Flight Center, Greenbelt, Maryland. Mr. R. L. Wright of the Goddard Space Flight Center was the Contracting Officer.

ABSTRACT

The investigation of materials specifically for solar cell applications has as its objective the improvement of solar energy conversion efficiencies, especially for cells operating in high energy environments. Silicon containing lithium as an impurity to interact with radiation damage centers was the principal material investigated. Solar cells having the n-on-p as well as p-on-n structures were prepared and radiation tested (NAS5-9131, RCA, Princeton). Prototype p-on-n cells having lithium in concentrations of the order of 5×10^{17} atoms per cc in the n-region have shown improved resistance to high energy electron bombardment. At a dosage of 10^{15} 1 MeV electrons per sq. cm, as high as 93% of the pre-irradiated short-circuit current was retained, compared to 77% for conventional 10 ohm cm n-on-p cells.

A second material investigated was aluminum antimonide. The zinc and cadmium diffused p-on-n structure which was investigated resulted in cells having efficiencies limited to about 1%, air mass one. It was concluded that suitably formed junctions less than 1 micron deep would be required for high conversion efficiencies. However, this was too shallow to be achieved with sufficiently high doping concentrations using either zinc or cadmium.

Various mathematical representations of the processing and irradiation effects were made throughout the program. This permitted defining the range of processing variables necessary to give required characteristics and predicted post-irradiation performance of the cells.

TABLE OF CONTENTS

TABLE OF CONTENTS (Continued)

LIST OF FIGURES

LIST OF FIGURES (Continued)

LIST OF FIGURES (Continued)

TABLES

SYMBOLS

α_λ	Absorption coefficient for wavelength λ	cm^{-1}
β	$= X/2\sqrt{Dt}$	
η	Output efficiency	percent
λ	Wavelength	microns
$\lambda_{\frac{1}{2}}$	Wavelength at which response is one-half the maximum, corresponding to the absorption edge of the material	microns
$\lambda_{max.}$	Wavelength at which the response is maximum	microns
μ	Mobility: or 10^{-4}cm, micron	cm^2/volt-sec
$\bar{\mu}$	Average mobility	cm^2/volt-sec
$\bar{\mu}$	Average mobility in the incremental distance	cm^2/volt-sec
ρ	Resistivity	ohm-cm
r	Minority carrier lifetime	micro-seconds
σ	Conductivity	mhos/cm
$\Delta\sigma$	Incremental conductivity	mhos/cm
ϕ	Integrated radiation flux	$/cm^2$
e, q	Electronic charge	coulomb
g_o	Carrier generation rate due to illumination	#/cc-sec
i	Subscript, "initial"	
j	Subscript, "junction"	
k	Boltzman's constant 1.38×10^{16}erg/deg	erg/deg
ℓ or x	Depth	cm
$\Delta\ell$ or Δx	Incremental distance	cm
n	Empirical recombination factor in diode equation	
$\bar{n}$	Average impurity concentration in incremental distance	#/c.c.

SYMBOLS (Continued)

q	Electronic charge	coulomb
t	Diffusion time	minutes
w	Optical penetration depth	cm
x	Depth	cm
x_j	Junction depth	cm
A	Area of cell or (depending on context) Acceptor concentration (permanent)	cm^2 /cc
B	Boron concentration	/cc
D	Diffusion constant (of impurities)	in^2/min or cm^2/sec
Eg	Energy gap	electron volts
I	Optical intensity at depth w , or (depending on context) Diode current	$/cm^2$ mA
I_L	Diode current due to photogenerated carriers	mA
I_o	Reverse saturation current of diode	mA
I_{sc}	Short-circuit current	mA
I_1/I_2	Ratio of short-circuit currents at conditions (1) and (2) or (depending on context) Ratio of currents at operating voltages V_1 and V_2	
K	Defect generation rate due to irradiation, according to $(1/L_f)^2 = (1/L_i)^2 + K\phi$	
K_1, K_2	Differences in absorption coefficients	/cm
L_i	Diffusion length of minority carriers, before irradiation	cm
L_f	Diffusion length of minority carriers, after irradiation	cm

SYMBOLS (Continued)

N	Donor concentration	$/cm^3$
N_n	Concentration of added impurities at distance x_j	$/cm^3$
N_o	Concentration of impurities at surface	$/cm^3$
R	Series resistance	ohms
T	Temperature	degrees Kelvin
V_{oc}	Open-circuit voltage	volts
V_1, V_2	Arbitrary voltages (1) and (2)	volts

MATERIALS DEVELOPMENT FOR SOLAR CELL APPLICATIONS

FINAL REPORT

Contract NAS5-9576

I. INTRODUCTION

This report covers the research and development work completed under contract NAS5-9576, "Materials Development for Solar Cell Applications". The objectives of the twelve (12) month program, extending from 1 June 1965 to 31 May 1966, were the development and application of materials specifically for improving the efficiency and radiation resistance of solar cells. The two main areas investigated were (1) the development of silicon solar cells embodying the principle of ion-pairing of radiation damage with lithium to negate cell deterioration, and (2) the utilization of aluminum antimonide as a solar cell base material.

In the investigation of the interaction of impurities with radiation damage, both the n-on-p and p-on-n cell types require the development of specific processing techniques for the introduction of lithium in a manner compatible with good cell performance. Further, the actual effectiveness of the impurity, lithium, to minimize radiation induced degradation of the cell's performance must be evaluated. Processing methods have been successfully devised for accomplishing high efficiency p-on-n and n-on-p silicon solar cells containing lithium concentrations of 10^{15} to 10^{17} atoms per cc in their base regions. As a result of the lithium diffused into the basic p-on-n cell, its deterioration under 1 MeV electron irradiation was found to be considerably less than that of any of the other comparable types of silicon solar cells. The processing methods, cell performances, and results of radiation exposures, are described in Section II of this report.

The second major area of consideration in this program was the development of aluminum antimonide as a solar cell base material. Interest in this material arises from its near optimum energy gap for conversion of solar energy. Its high reactivity to oxygen and moisture has not been a specific deterrent in the formation of photovoltaic junctions. Work in the present program has established that the diffusion conditions necessary to form junctions of adequately low sheet resistance also produce junctions of greater than 2-3 micron depth. An analysis based on the optical absorption properties of aluminum antimonide predicts that the junction depth must be restricted to less than 1-2 microns in order to realize appreciable conversion efficiencies of solar radiation. To date this has not been found technically possible using the diffusants zinc or cadmium. The junction and cell properties established during this program, and various evaluation methods, are summarized in Section III of this report.

Since the lifetime, or diffusion length, of minority carriers in the base region of solar cells is the basic property affected by irradiation, it would be anticipated that improvement in pre-irradiation lifetimes would reduce radiation damage. In this program it has been established that various thermal treatments are feasible which would at least double the initial carrier lifetimes in the cells. However, the improved performance under irradiation, achieved by increasing the initial lifetimes, is predicted to be less that that which is currently realized by incorporating lithium into the p-on-n cells. These findings are reported in Section IV of this report.

II. SILICON SOLAR CELLS CONTAINING LITHIUM AS AN INTERACTING IMPURITY

A. Introduction

The interaction of lithium with radiation-induced damage centers has been established as, for instance, References 1 and 2. Application of this principle to reduce the deterioration of solar cells exposed to high energy radiation was undertaken in the present program. The objective has been to establish the concentrations of lithium which are sufficient for ion-pairing with the damage centers, yet maintain cells of high efficiency. These concentrations should give resistivities which are compatible with the usual solar cell types; i.e., in the range 1 to 15 ohm cm. Higher or lower resistivities adversely affect the efficiencies of the cells, either by reducing the voltage, as in the case of high resistivities, or reduced short-circuit currents in the case of low resistivity. For n-on-p cells, these considerations imply starting with p-type material of low resistivity. Since the acceptors themselves form complexes with lithium, Reference 3, the probability of the lithium interacting with radiation damage centers is considerably reduced the lower the initial resistivity (hence, higher donor concentration).

In the case of p-on-n type cells, the converse is true. Sufficiently high concentrations of lithium to give a good probability of interaction with the radiation damage centers result in low base resistivities and, consequently, low currents.

The pre- and post-irradiation performance of n-on-p and p-on-n silicon cells having lithium diffused in the base region is given in the following sections.

B. N-on-P Silicon Solar Cells, Lithium Diffused P-Region

The development of the lithium-doped n-on-p type silicon solar cells has covered the following aspects:

1. Process Development and Analytical Representation.
2. Cell Types Fabricated and Performance.

1. Process Development and Analytical Representation.

It was early established that diffusion of lithium into n-type silicon did not readily produce uniform lithium distributions. Moreover, to obtain uniform distributions in the base required long "drive-in" times. The amount of lithium introduced for ordinary conditions (300 to 400°C, greater than 2 minutes) gives excessively high resistivities. The process utilized was developed under separate RCA funding (Reference 4) and is outlined in Figure 1. The procedure of removing part of the initially diffused lithium layer prior to the drive-in or redistribution cycle facilitates controlling the final concentrations to the desired amounts; i.e., resistivities in the range 0.5 to 15 ohm cm.

Lithium Diffusion Procedure: After the silicon surface is etched using standard solar cell fabrication procedures, it is coated with a 30% lithium, 60% mineral oil, 1% oleic acid suspension. The lithium diffusion is then performed in a forming gas atmosphere for the specified times and temperatures. The remaining excess lithium is then removed by physically wiping, followed by physically removing part of the diffused layer by etching in HF : HNO_3 or by lapping.

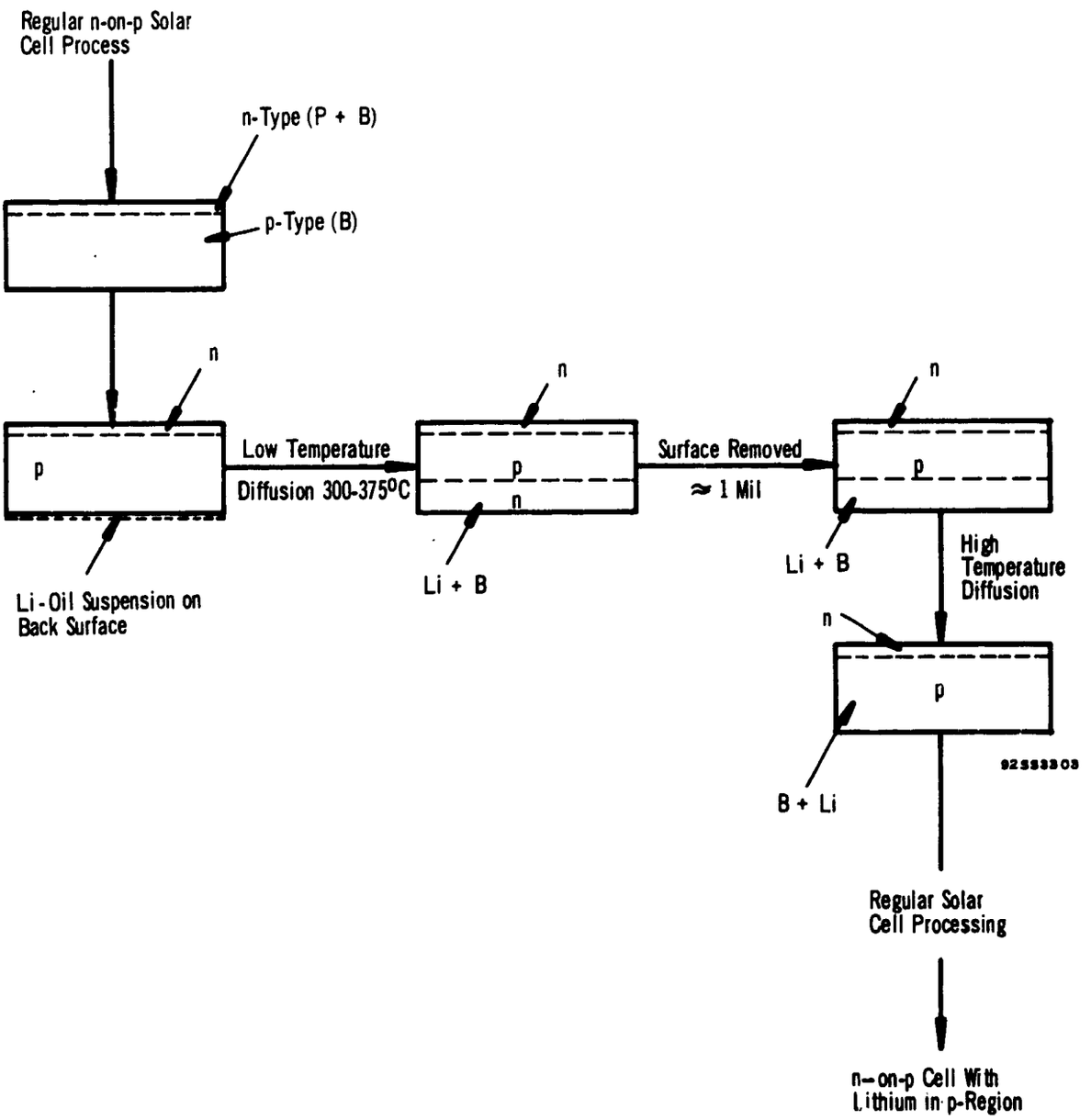

FIGURE 1. LITHIUM INTRODUCTION PROCESS FOR N-ON-P CELLS

Cell Fabrication Procedure The n-on-p lithium doped solar cells were fabricated by standard procedures except that after the phosphorus diffusion to form the n/p junction, and removal of the n skin from the back surface of the cell, the lithium is diffused into the cell by the procedures described above.

The lithium diffusion parameters principally investigated were 30 to 120 minute diffusion times at 300°C. The portion of the diffused surface removed prior to the drive-in step was generally 1 mil. The lithium redistribution cycle was standardized at 400°C for 30 minutes.

Analytical Representations

In the development of n-on-p lithium doped solar cells, basically two representations of the process are necessary. One is the distribution of a diffused impurity, or impurity profile. The second is the final concentration of doping to be expected for the particular three-step process described above, where part of an initial diffused layer is removed, and the remaining dopant is redistributed in the bulk. The methods of characterizing, measuring, and predicting these processes are described below.

The method employed for determining the distribution of diffused lithium is to successively remove thin sections of the silicon and measure the sheet resistance of the remaining

portion of the wafer. The sheet conductivity of the layer removed is given (Reference 5) by

$$\Delta\sigma = q\bar{\mu}\left[N_o \left\{ Ax - (\Delta x)^2/2\sqrt{Dt} \right\} - A\Delta x \right]$$

The assumptions are that the impurity doping follows an error function distribution, that the value of $x/2\sqrt{D\,t}$ is small compared to unity (permitting a series approximation of the error function), and all the lithium is ionized at room temperatures except for a small fraction equal to the original doping of the bulk.

The value of N_n at the surface after removal of a given layer is readily determined from

$$N_n = N_o \ \text{erfc} \ x_j \ /2\sqrt{D\,t}$$

where N_n is the concentration at the distance x_j from the surface.

A simpler representation of the change of measurable parameters of a lithium diffused layer is obtained by considering the diffused profile to be a series of layers each homogeneous in itself, but of different impurity concentrations. Then a sheet conductivity measurement is a summation of the incremental conductivities. Therefore, on the removal of a surface layer, the conductivity of that layer is

$$\sigma_\ell = \sigma_1 - \sigma_2 = \bar{n}_\ell \, q \, \bar{\mu}_\ell \, \Delta\ell$$

In both of the preceding representations of the incremental sheet conductivity the mobilities are assumed independent of the particular species of dopant, and are for n-type silicon, (Reference 6)

$$\mu = 300\ (19-N) \text{ for } 10^{16} < N < 5\times10^{18}/cc$$

or

$$\bar{\mu} = 5700 - 150 \log N_o^2\ (\text{erfc}\ x_1/\ 2\sqrt{Dt})(\text{erfc}\ x_2/\ 2\sqrt{Dt}\ )$$

Figure 2 is a plot of both of the foregoing representations, giving the calculated sheet conductivity change versus concentration. The differences between the curves A and B are not considered excessive considering the estimated values of N and D . The actual doping profile of lithium diffused silicon can be determined from these curves.

The above analysis was used to predict the sheet conductivity versus depth. Figure 3 gives the results of this type of calculation and for comparison, the data for a 42 minute diffusion at 300°C is also given. The values of the diffusion constant, D , and surface concentration, N , as used in the calculations were determined as described in the respective sections "Lithium Diffusion Constant" and "Surface Concentration of Lithium".

The above is readily extended to the prediction of the results of the three-step procedure devised for incorporating the lithium into the regular n-on-p structure. The three steps

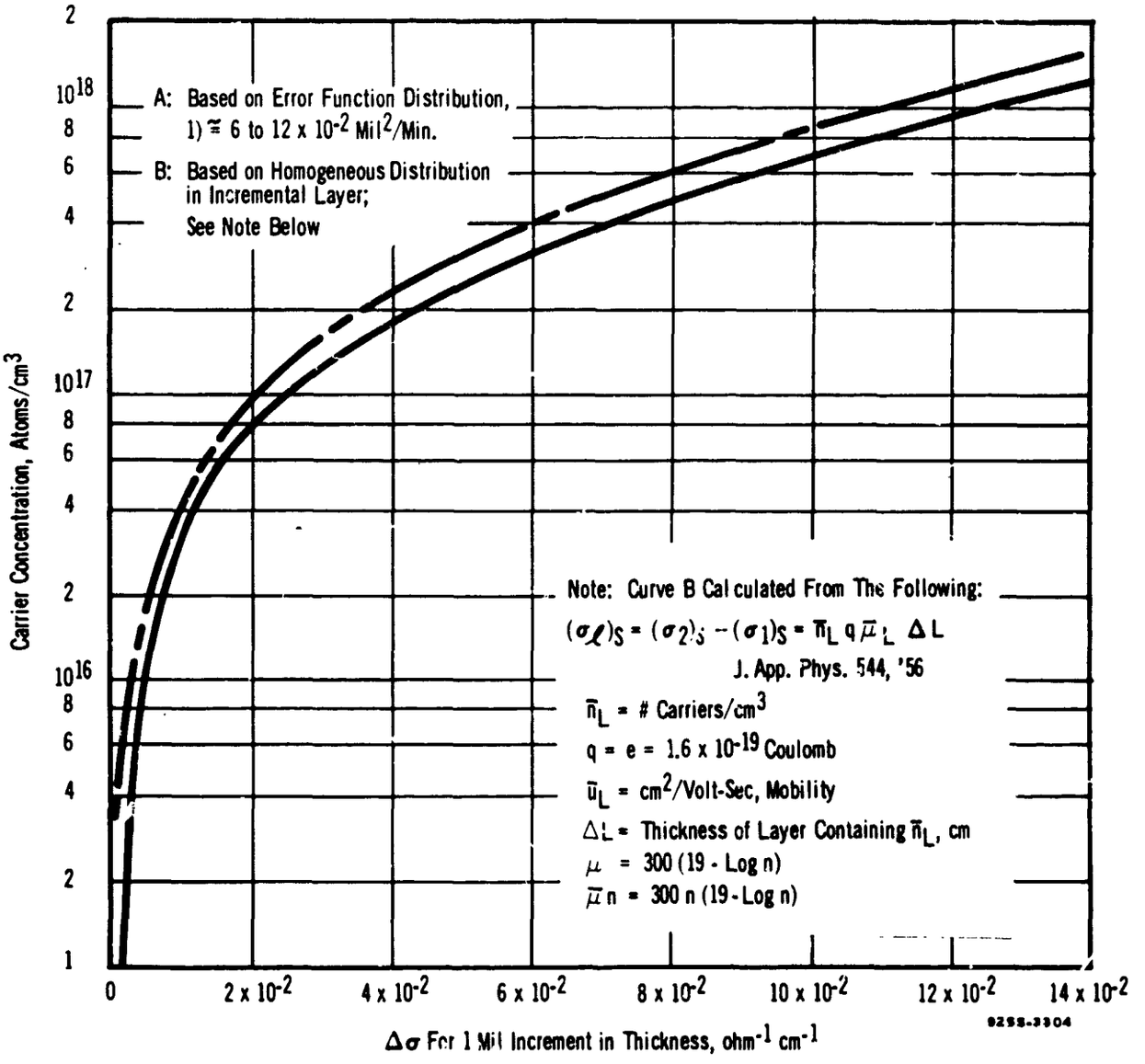

FIGURE 2. COMPARISON OF SHEET CONDUCTIVITIES CALCULATED FROM ERROR FUNCTION AND HOMOGENEOUS IMPURITY DISTRIBUTIONS

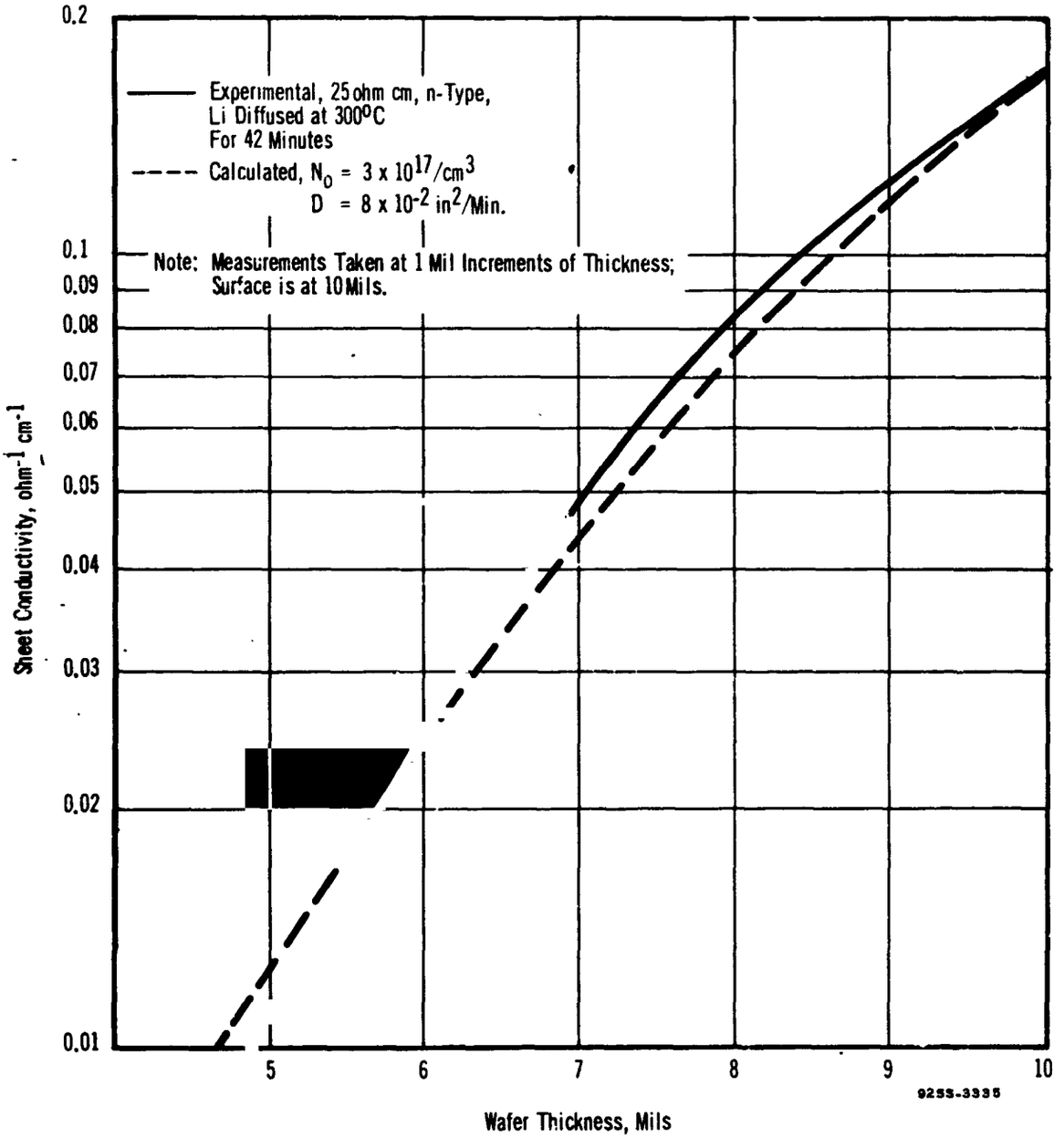

FIGURE 3. CALCULATED AND EXPERIMENTAL SHEET CONDUCTIVITY AS A FUNCTION OF DEPTH

are surface diffusion, removal of a portion of that surface, and a thermal treatment to redistribute the dopant throughout the bulk. The final concentration of lithium can be approximated using the assumptions that the dopant is distributed uniformly in the bulk, and the lithium diffusion constant is the same regardless of diffusion time. Thus, since the resistivity is proportional to the net doping,

$$\rho = 1/q\mu(N-A)$$

The donor concentration remaining in that portion of the diffused surface not removed by surface lapping is

$$N = (N_o/\ell) \int_{x_1}^{x_2} \operatorname{erfc} \beta \, d\beta$$

where ℓ is the thickness remaining, $\ell = x_2 - x_1$

$$\beta = x/2\sqrt{Dt}$$

The resistivity is then readily determined from (N - A). No complexing or precipitation processes are considered in this prediction. The final resistivity as a function of diffusion time, calculated for several variations of the possible tolerances in the dimensions encountered in the processing, is given in Figure 4. Applicable diffusion times for the case of surface removals of 1 mil would therefore be about 70 to 90 minutes to achieve base resistivities of the order of 7 to 15 ohm cm for 1 ohm cm starting material.

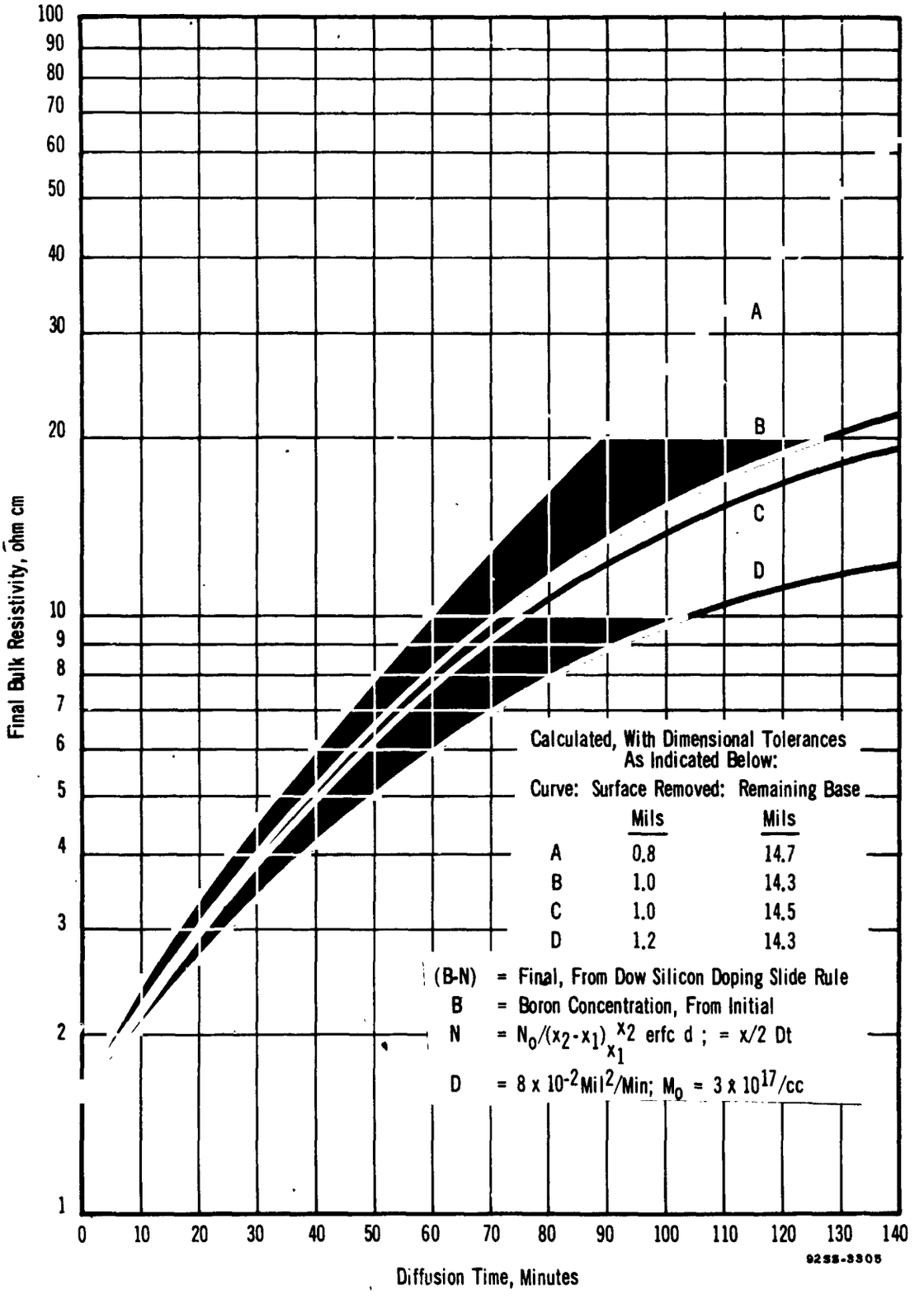

FIGURE 4. PREDICTED FINAL BULK RESISTIVITY AS A FUNCTION OF SURFACE DIFFUSION TIME

Lithium Diffusion Constant: The diffusion constant for lithium in silicon has been published (References 3,7) as 0.93×10^{-2} sq. mil/min. Experimentally, the diffusion constant was determined as 8×10^{-2} sq. mil/min. This was based on the calculation of the diffusion constant from

$$x_j \cong 2\sqrt{Dt}$$

for 300°C diffusions for respectively 42 and 60 minutes into 25 ohm cm p-type silicon. The difference between the experimental value and the published value is not considered excessive.

Surface Concentration of Lithium: Basically four methods were used to estimate the surface concentration (solid solubility) of lithium in silicon. These methods and the subsequent values of solid solubilities as determined for 300°C were

a. Junction depth: (3.4×10^{18} per cc): The error function distribution gives the bulk concentration at the location where the diffused doping and the bulk doping are equal, or

$$A = N_o \operatorname{erfc} x_j / 2\sqrt{Dt}$$

For 25 ohm cm p-type silicon the bulk doping of 5.4×10^{14} per cc is equalized at depths (junction depths) of 10 to 12 mils for diffusion times of 42 and 60 minutes respectively. The diffusion constant of 8×10^{-2} sq. mil per min. was used in the computations.

b. Empirical fitting to the measured sheet conductivity profile, assuming various surface concentrations, (3×10^{17}/cc), as indicated in Figure 3 .

c. Determination from the incremental sheet conductivity and using Figure 2. (1.8 to 2.2 x 10^{17}/cc).

d. Base resistivity for sufficiently long diffusion times to produce saturation (1.5×10^{16}/cc).

The value of 3×10^{17}/cc was considered the best tentative estimate for diffusion into p-type material of the resistivity range 1 to 25 ohm cm.

2. Cell Types Fabricated and Performance

The three-step process was found to give the base resistivities shown in Figure 5 for the range of diffusion times shown. A 300°C surface diffusion, removal of 1 mil of the lithium diffused surface, and a 400°C - 30 minute redistribution cycle were consistently used. What appears as reduced lithium concentrations with increased diffusion times greater than 80 minutes was attributed to complexing or precipitation reactions of the lithium. Based on the results of Figure 5, the following categories of cells were fabricated.

a. 10 ohm cm, Czochralski grown, with a lithium doping estimated as 5×10^{14}/cc.

b. 1.5 ohm cm, float-zone grown, doping estimated as 5×10^{15}/cc.

c. 1.5 ohm cm, float-zone grown silicon, doping estimated as 9×10^{15}/cc for free lithium.

d. 2.5-2.8 ohm cm, float-zone grown silicon, doping estimated as 5×10^{15}/cc.

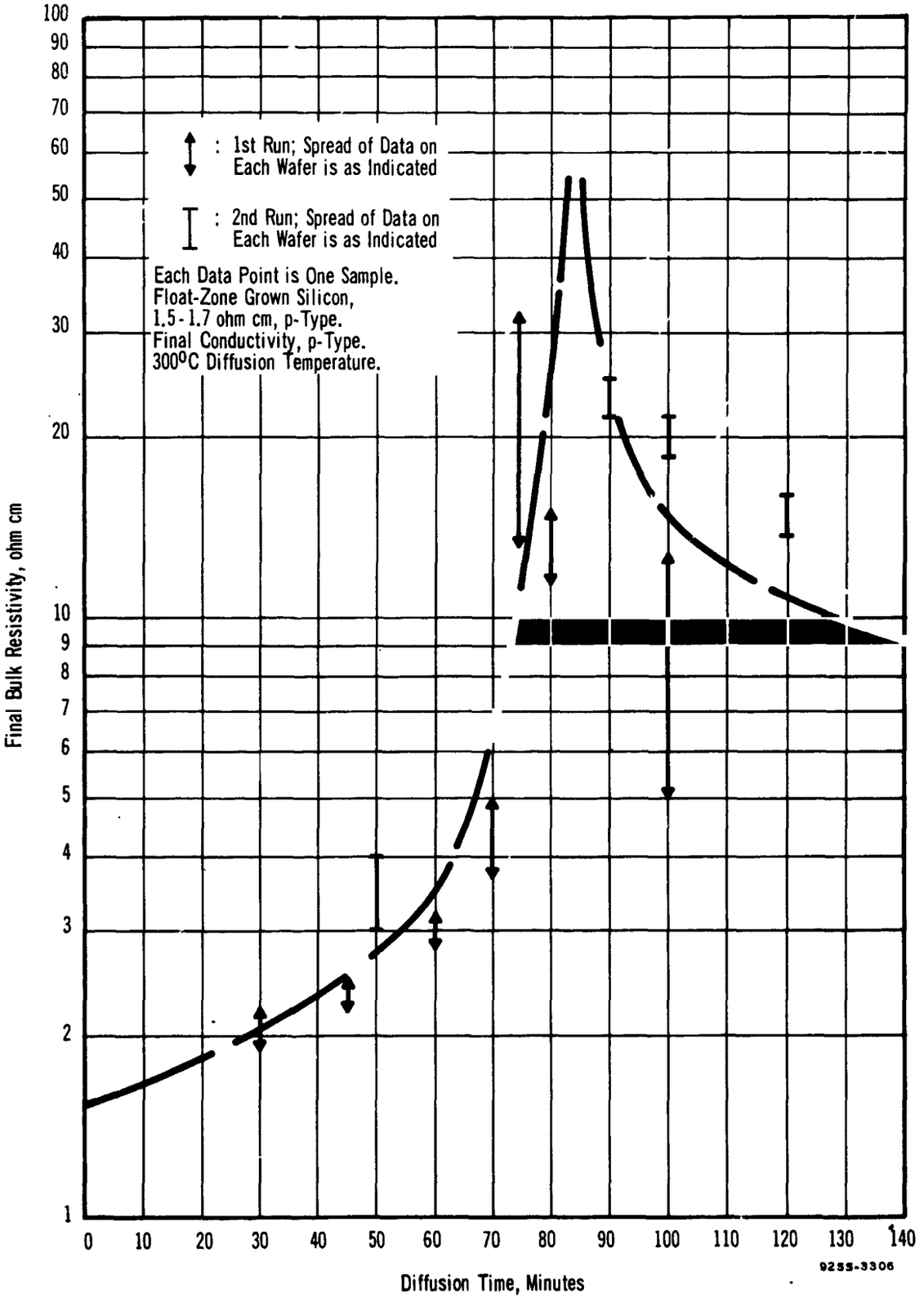

FIGURE 5. EXPERIMENTAL FINAL BULK RESISTIVITY AS A FUNCTION OF SURFACE DIFFUSION TIME

The basic parameters and performance of these cells are given in Table I. It is apparent that lithium does not adversely affect the attainable efficiencies. Also, it is concluded that not only has the process per se failed to introduce lithium in substantial concentrations within a diffusion length of the junction, but it is not of sufficient concentrations to affect the radiation damage results.

The voltage-current characteristics of representative cells from these groups are given in Figures 6 and 7. The effect of decreasing the current and increasing the open-circuit voltage as the base resistivity decreases is generally apparent in these cells, which would indicate the progressive increase in lithium concentration effected with the changes in processing.

The degradation produced by 1 MeV electrons has been evaluated as summarized in Table I. The minority carrier diffusion lengths after 10^{15} 1 MeV electrons/cm^2 for the cells containing lithium ranged from 28 to 37 microns for the types tested. This is considered within the range characteristic of 2 to 10 ohm cm conventional n-on-p cells, namely 24 to 32 microns. It is concluded that any radiation resistance differences noted for the various amounts of lithium incorporated in the n-on-p cells is more a characteristic of the resulting variation in base resistance than attributal to damage center-impurity interaction.

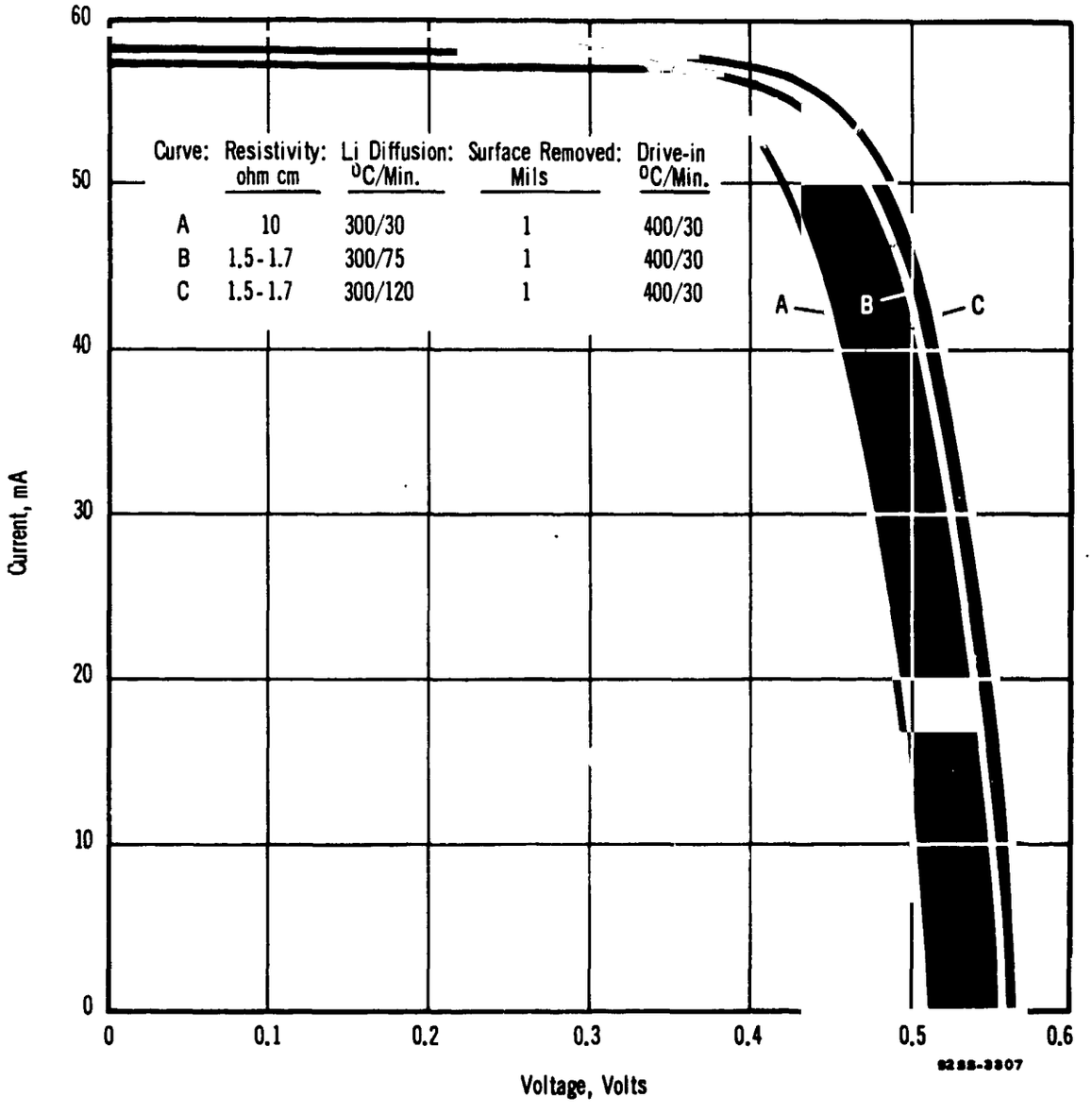

FIGURE 6. VOLTAGE-CURRENT CHARACTERISTICS OF SILICON N-ON-P SOLAR CELLS, LITHIUM DIFFUSED INTO P-REGION

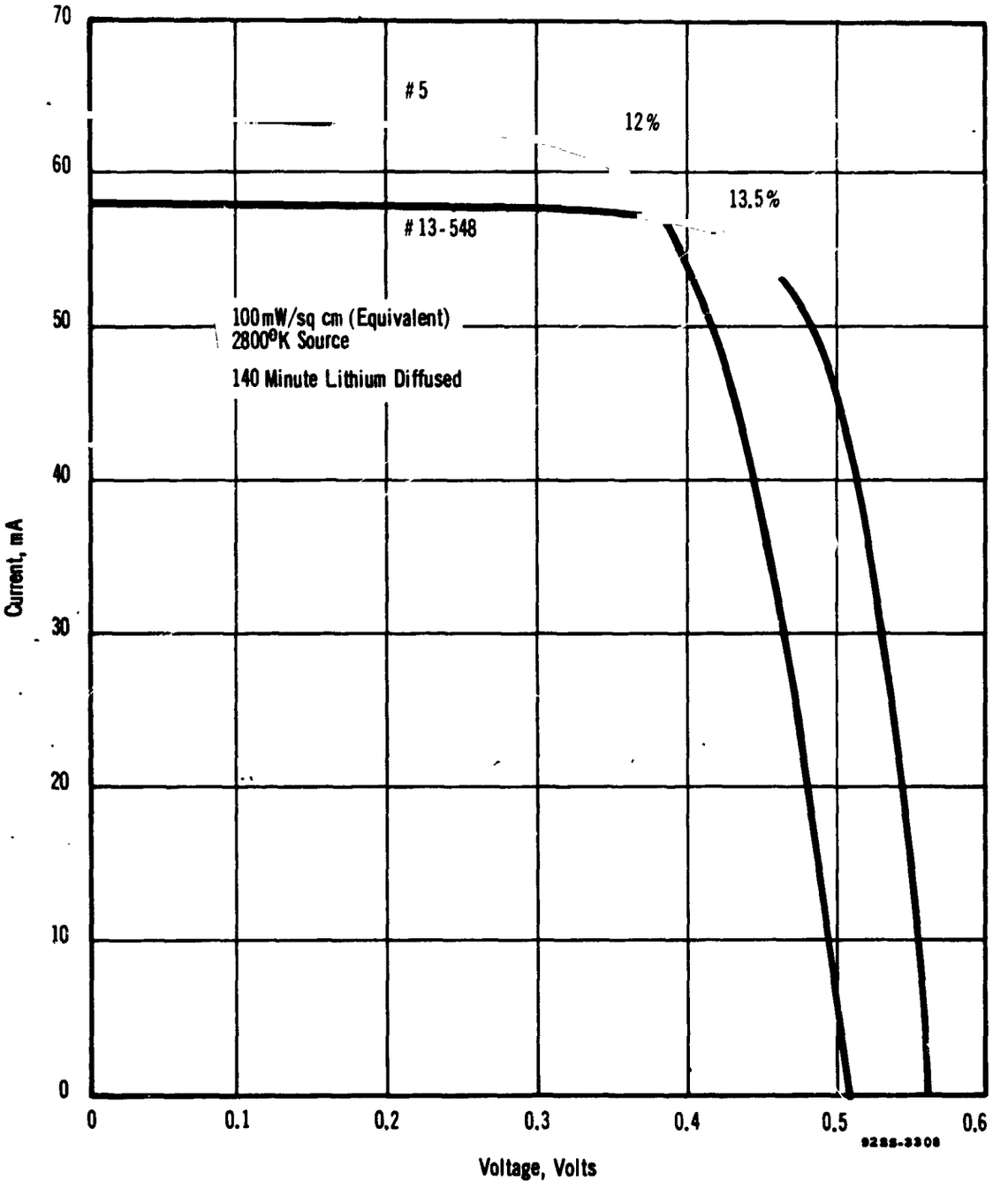

FIGURE 7. VOLTAGE-CURRENT CHARACTERISTICS OF SILICON N-ON-P SOLAR CELLS, LITHIUM DIFFUSED INTO P-REGION

TABLE I

COMPARISON OF RADIATION DAMAGE OF VARIOUS TYPES OF N-ON-P CELLS HAVING LITHIUM DIFFUSED P-REGION

Initial Resistivity ohm-cm	1.5	1.5	10	2.5-2.8	10	2
Crystal Type	F.Z.	F.Z.	Q.C.	F.Z.	Q.C.	Q.C.
Final Resistivity ohm-cm	3-25	15-18	13-15	16-18	10	2
Li, est. from ρ	5×10^{15}	9×10^{15}	5×10^{14}	5×10^{16}	none	none
V_{oc}, volts	.54-.56	.55-.57	.49-.51	.508, .509		
I_{sc} mA	54.5-59	55-59	56-59	62.5, 63.5		
η (max.) = percent	13.3	13.9	11.9	12, 12.4		
Li Diffusion Time minutes	75	120	30	140		
Li Re-Dist. Time minutes	30	30	30	60		
Carrier Lifetime microseconds		3-8	15-25	0.7-1.7		
τ_i (microns)		150	190	170	130	163
τ at $\phi = 1 \times 10^{15}$ (microns)		37	32	28	32	24
References:	-	-	-	-	1	2

1, page 26
2, page 30

C. P-On-N Silicon Solar Cells, Lithium Diffused N-Region

1. Performance of P-On-N Cells

P-on-n cells having a lithium diffused n-region were prepared from silicon having a broad range of initial properties. The pre-irradiated average photovoltaic performance of the various classes of cells is given in Table II. The products of $I_{sc} \times V_{oc}$ show that a wide range of conditions yields the approximately same final cell efficiency. Thus, no specific silicon, either with respect to original growth mechanism, conductivity type, or resistivity, appears to be the factor critically affecting the efficiencies of the cells.

Of particular note for the p-on-n type cell is the relatively low lifetimes as illustrated in Table II compared to that obtained for n-on-p cells. This problem is related to several factors, such as the relative compensation used in the initial silicon or the effects of heavily doping with lithium.

Typical V-I photovoltaic curves of the various categories of cells are given in Figures 8, 9, and 10. While the averages of the cells, as illustrated in Table II, give cells of potentially nearly equal efficiencies, a wide spread in individual cell performance is evident. The factor limiting the current appears to be the relatively low minority carrier lifetimes experienced with these particular groups of p-on-n cells. It is to be noted that the unusually high open-circuit voltages of 0.595 volts were obtained under extreme differences in starting materials, namely for 16-18 ohm cm n-type as well as 100 ohm cm p-type, both float-zone.

TABLE II

PERFORMANCE OF P-ON-N CELLS

Starting Material			V-I Performance (Averages)				
Conductive Type	Growth Method	ρ ohm cm	I_{sc} ma	V_{oc} volts	Calc. From Averages $(I_{sc})(V_{oc})$ %	η max. $(0.41)(I_{sc}V_{oc})$ (2) %	Lifetime $\bar{\tau}_i$ μsec
n	F.Z.	16-18	49.5	.575	28.4	11.7	1.0-5.0
n	Lopex	12.5	49.5 (1)	.525	26.0	10.8	0.5-1.5
n	F.Z.	10	49.5	.585	29.0	12	0.3-1.5
p	F.Z.	100	50.2	.565	28.4	11.7	0.6-2
p	F.Z.	50	48.3	.590	28.5	11.8	2.5-4.0
p	C.G.	25	54.4	.590	32.1	13.1	3 -10

Note: (1) 12.5 ohm cm cell size 0.24 x 0.24 inch; : current as listed calculated for 1 x 2 cm size; voltage of 0.525 for 0.24 x 0.24 size but would be higher for 1 x 2 cm size.

(2) Fill factor of 0.41 used as corrective value to estimate efficiency obtainable from "average" cells. For n-on-p, 1 x 2 cm, 1 ohm cm cells, fill factor of 0.43 is characteristic of 13% efficiency.

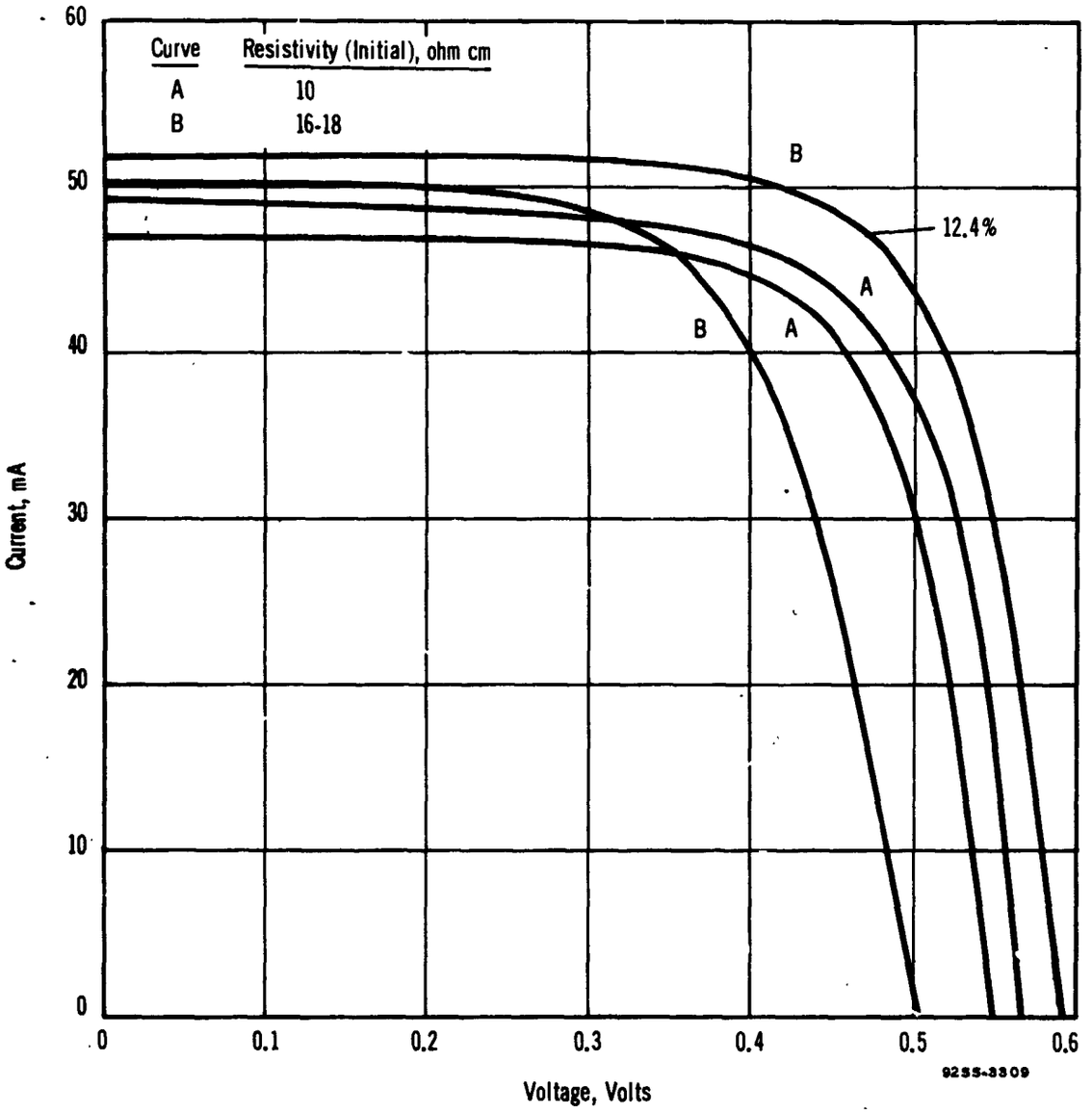

FIGURE 8. VOLTAGE-CURRENT CURVES REPRESENTATIVE OF P-ON-N CELLS, 16-18 OHM CM (n) AND 10 OHM CM FLOAT ZONE STARTING MATERIAL

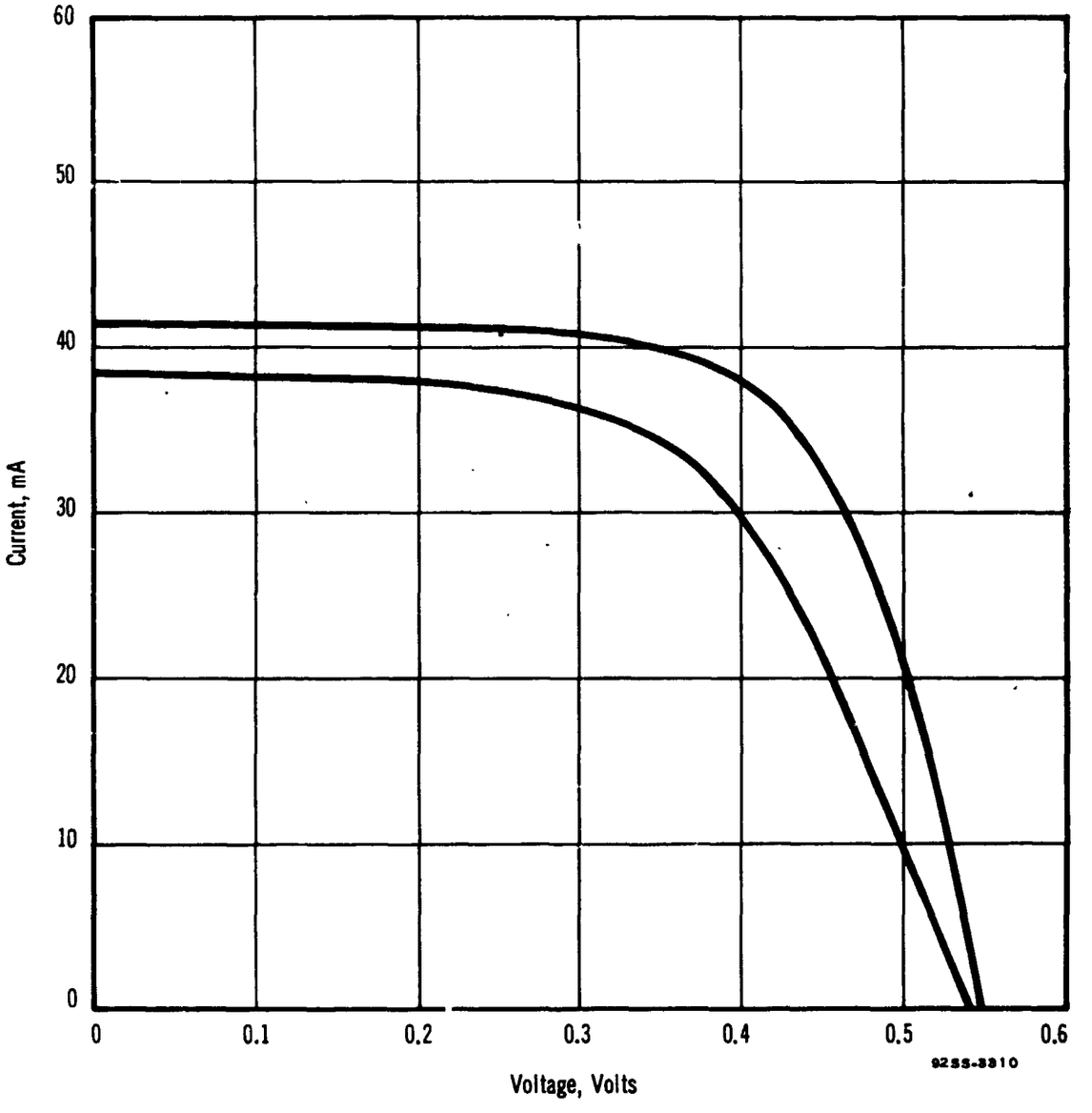

FIGURE 9. VOLTAGE-CURRENT CURVES REPRESENTATIVE OF P-ON-N CELLS, 12.5 OHM CM (n) LOPEX STARTING MATERIAL

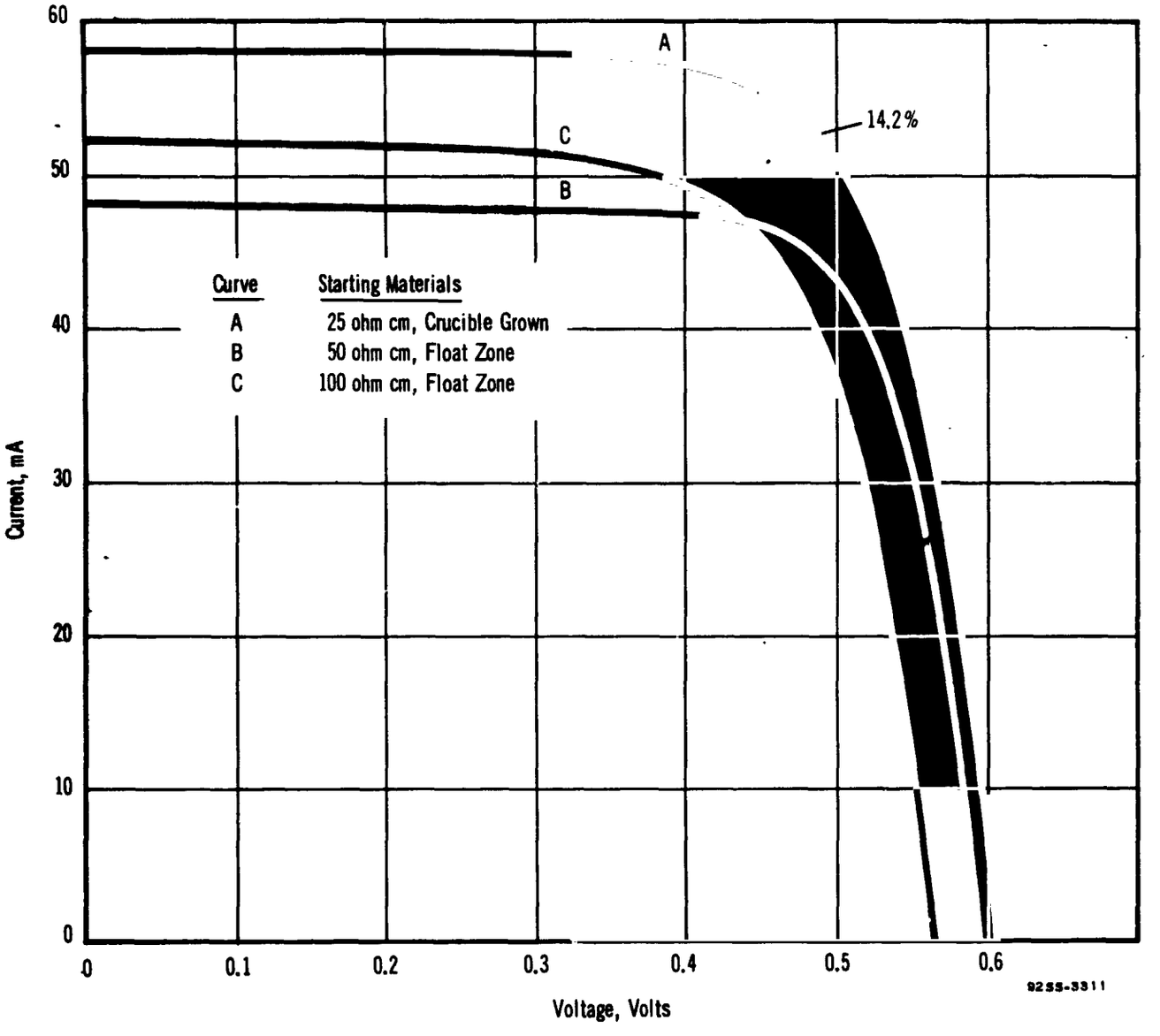

FIGURE 10. VOLTAGE-CURRENT CURVES REPRESENTATIVE OF P-ON-N CELLS, 50 OHM CM (p) AND 100 OHM CM (p) FLOAT ZONE STARTING MATERIAL

A very evident problem is illustrated in Figures 11 and 12. The irradiac curve characterized as "S"-shaped occurred for a few of the cells under two conditions, either after storage at room temperature or during silicon monoxide coating. Figure11 shows the effect of storage; the same type of change has been observed to occur during optical coating. Although the exact control of this effect has not been established, it is measurable as an increased series resistance and is removable by heat treatment as shown in Figure 12.

2. Radiation Damage Performance of P-On-N Cells

Irradiation tests have been made on representative cells by both the RCA Laboratories, Princeton, New Jersey, and NASA, Goddard Space Flight Center, Greenbelt, Maryland. It is expected these organizations will report their finds under separate cover. The following presents some of the early findings for 1 MeV electron irradiations performed at the RCA Princeton Laboratories.

Figure 13 presents the results of 1 MeV irradiations in terms of change in short-circuit current. The data points for individual cells at 8×10^{14}, 2×10^{15} and 10^{16} electrons/sq. cm show the improved resistance to high energy radiation realized for the lithium diffused p-on-n type silicon solar cells. The final values of short-circuit currents for the two cells irradiated to 10^{16}/sq. cm are given with that of a typical 10 ohm cm n-on-p cell. This illustrates that the lower percentage change of the p-on-n cells results in higher performance cells, even though their initial efficiencies are below those of

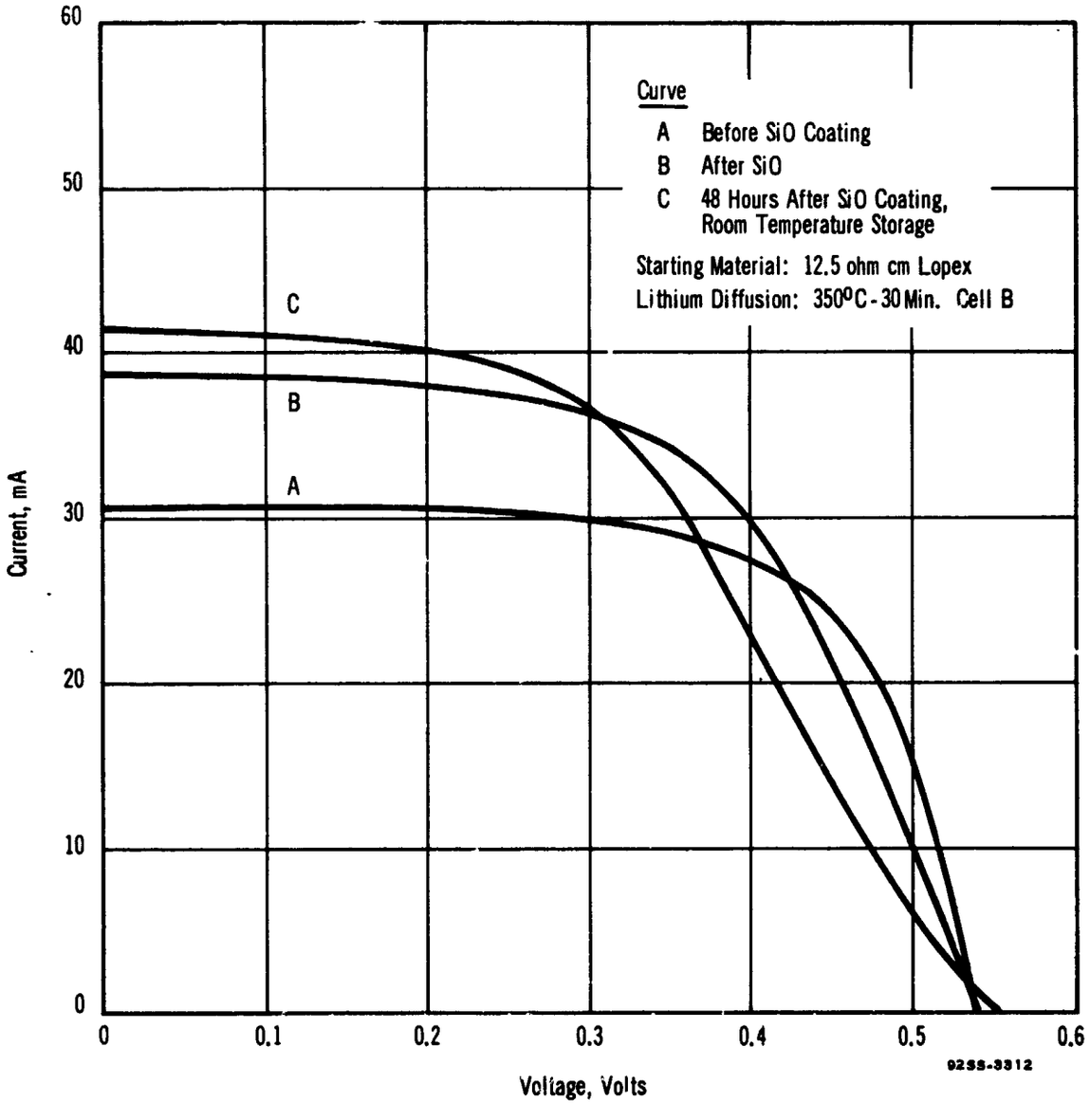

FIGURE 11. INCREASED SERIES RESISTANCE EFFECT IN P-ON-N LITHIUM DIFFUSED CELL

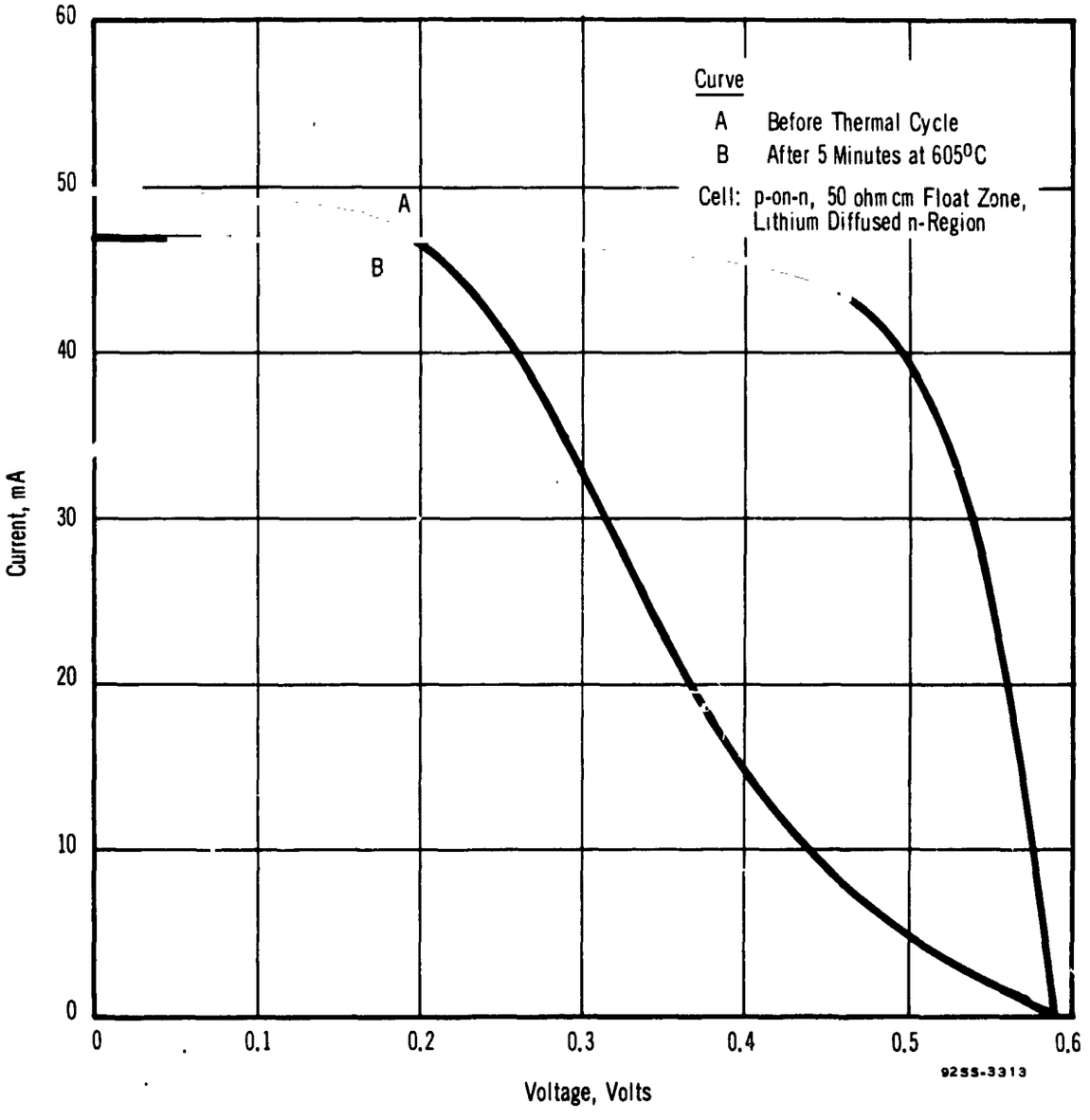

FIGURE 12. EFFECT OF THERMAL TREATMENT ON SERIES RESISTANCE

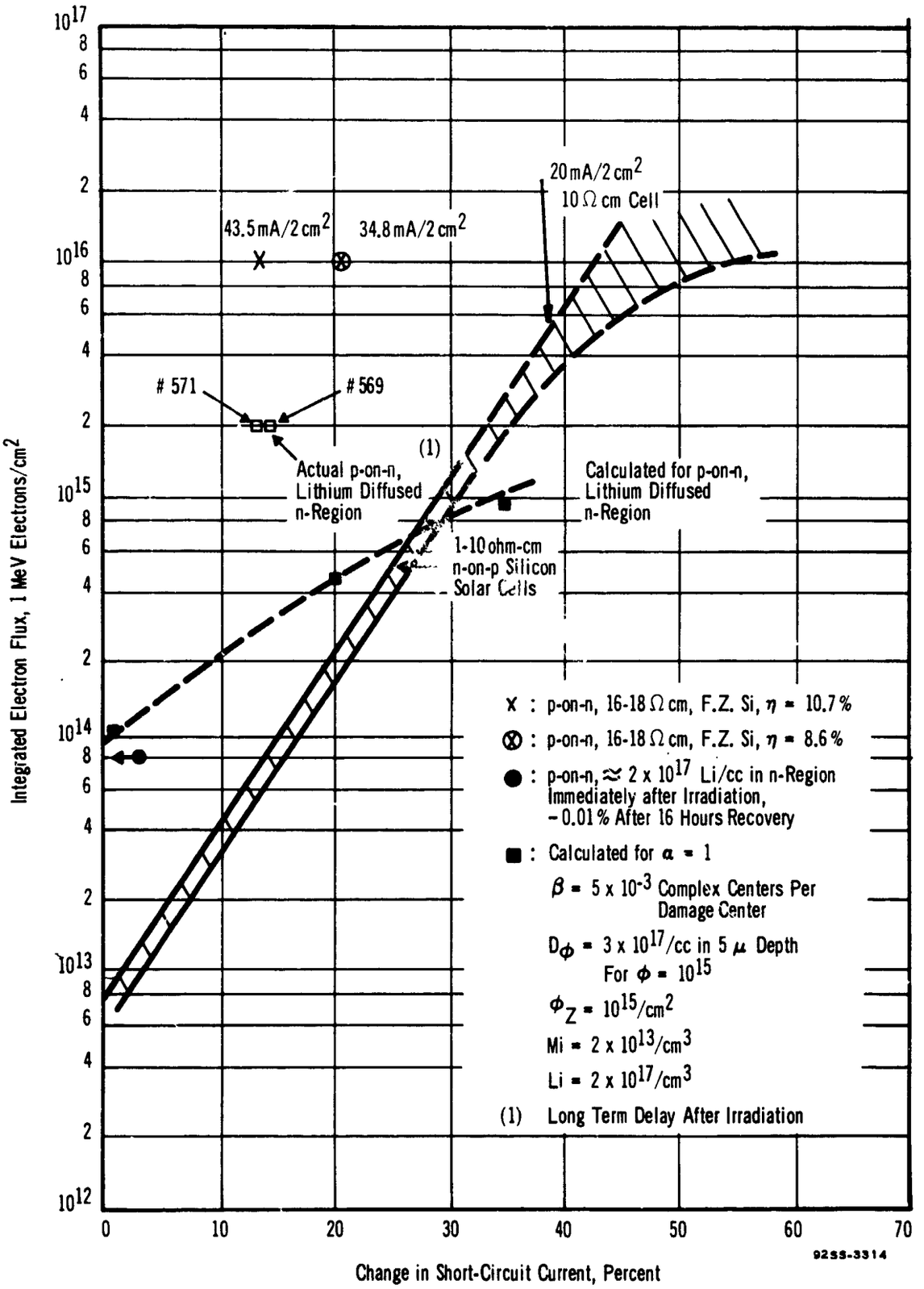

FIGURE 13. ELECTRON IRRADIATED SHORT-CIRCUIT CURRENT DEGRADATION OF SILICON P-ON-N SOLAR CELLS HAVING LITHIUM DIFFUSED N-REGION

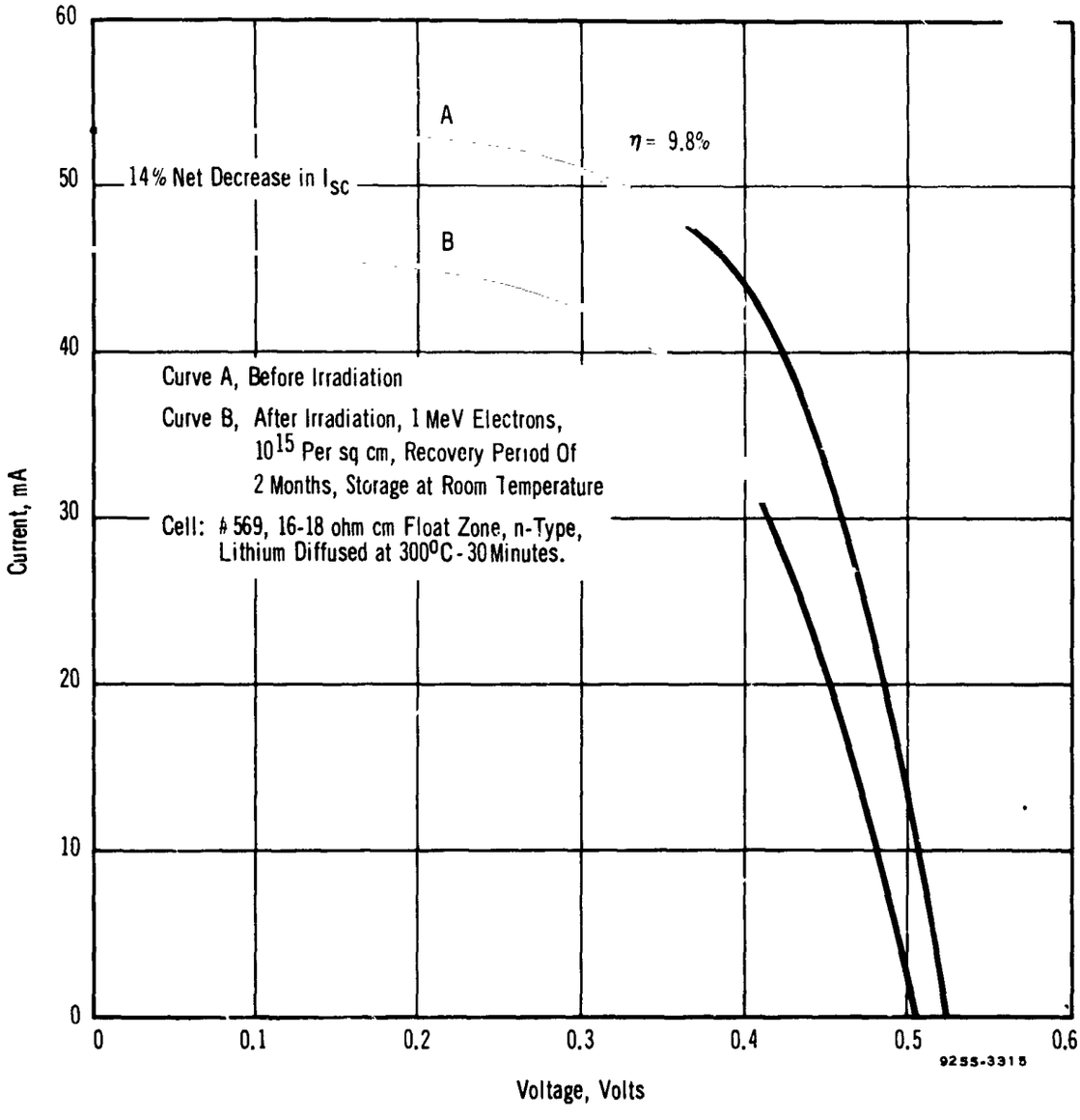

FIGURE 14. ELECTRON IRRADIATION EFFECT ON PHOTOVOLTAIC RESPONSE OF P-ON-N LITHIUM DIFFUSED CELL # 569

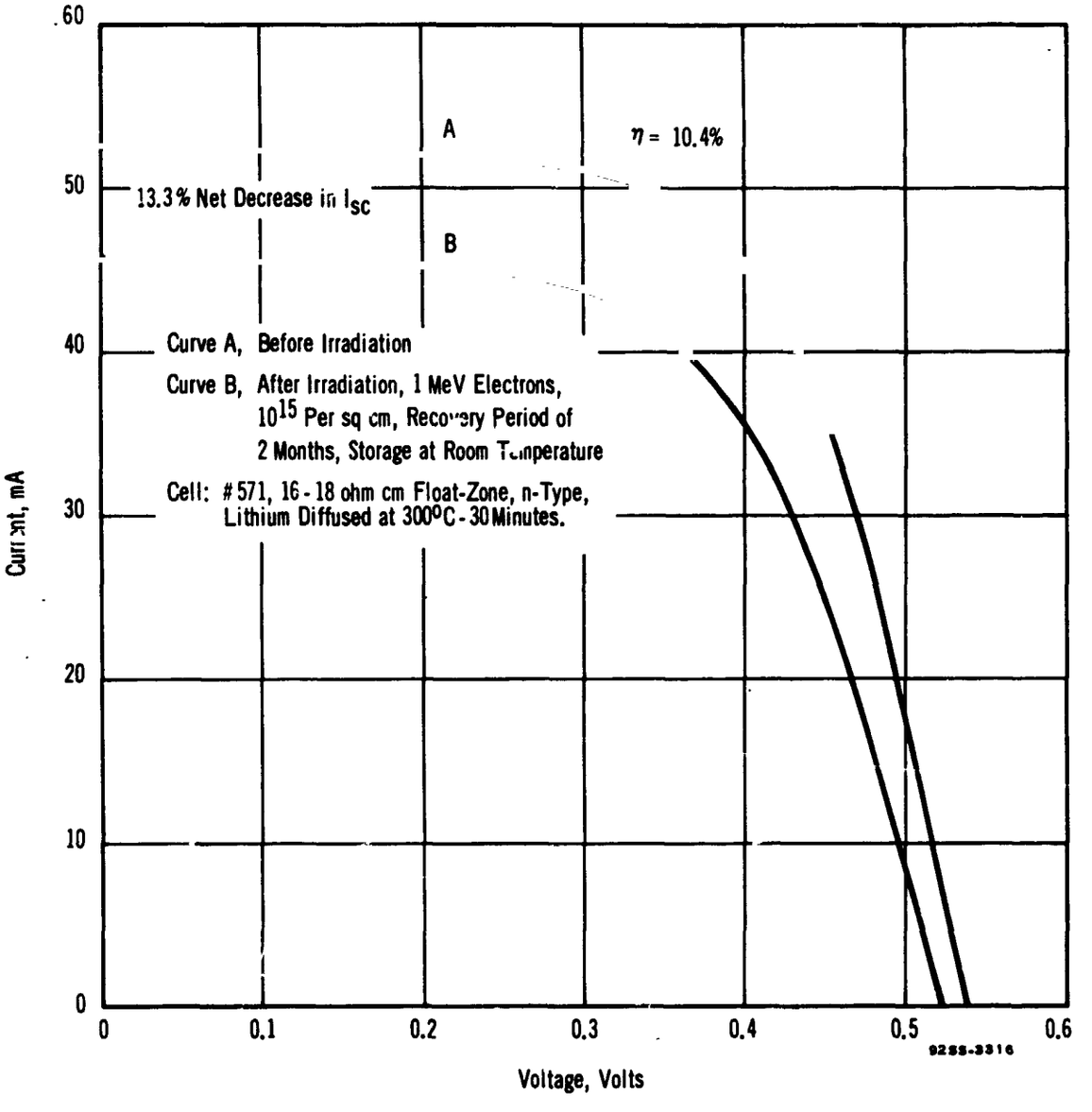

FIGURE 15 ELECTRON IRRADIATION EFFECT ON PHOTOVOLTAIC RESPONSE OF P-ON-N LITHIUM DIFFUSED CELL #571

typical 10 ohm cm n-on-p cells. The voltage-current curves for cells #569 and #571, before and after irradiation, are given in Figures 14 and 15. The time period for the recovery to occur in this instance was about two months; however, this is not typical. Recovery time was found (RCA-Laboratories, Princeton) to depend on irradiation rate and for cells prepared subsequent to the #569-#571 series, times of the order of minutes were observed.

3. Process Evaluation

The distribution of the performance characteristics of a group of 30 similarly processed cells was analyzed to evaluate the degree of process control achieved. The performance characteristics are summarized below:

	Average	Maximum	Minimum
V_{oc} (volts)	0.590	0.605	0.565
I_{sc} (mA)	54.4	58.0	51.2
η, percent, at 0.49 volt	12.9	14.2	10.1

The degree to which the data fits a normal distribution is evaluated, respectively, for V_{oc}, I_{sc}, η max. in terms of the linearity of the data plotted in Figure 16. Since the total number of cells is somewhat limited, the significance of the highest and lowest data groups can be minimized. As indicated by the linearity of most of the data groupings presented in Figure 16, the respective parameters have approximately normally distributed values. This demonstrates that reasonably good control has been achieved in the over-all processing of the p-on-n type cells, presupposing uniformly distributed properties of the starting silicon.

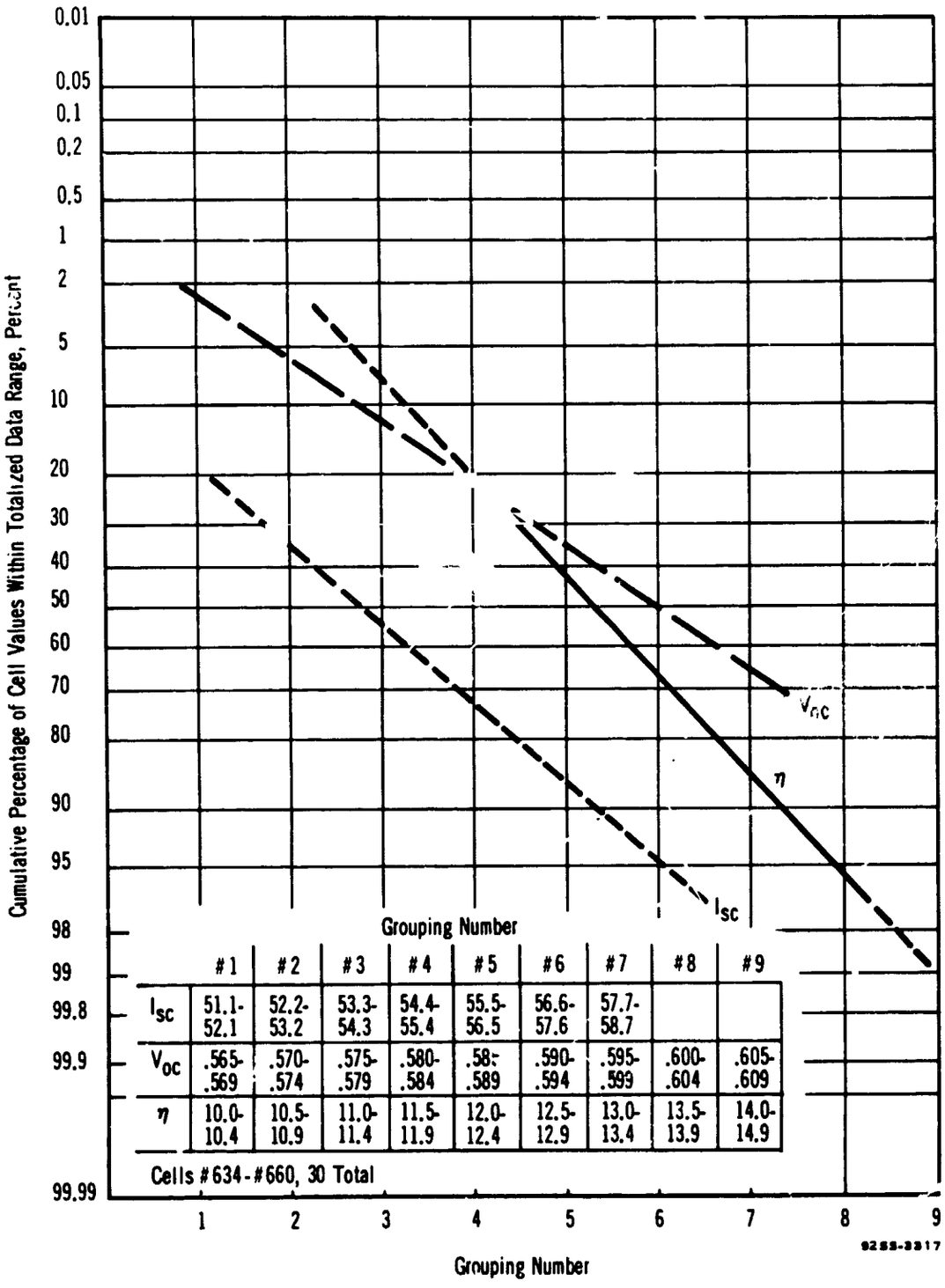

	#1	#2	#3	#4	#5	#6	#7	#8	#9
I_{sc}	51.1-52.1	52.2-53.2	53.3-54.3	54.4-55.4	55.5-56.5	56.6-57.6	57.7-58.7		
V_{oc}	.565-.569	.570-.574	.575-.579	.580-.584	.585-.589	.590-.594	.595-.599	.600-.604	.605-.609
η	10.0-10.4	10.5-10.9	11.0-11.4	11.5-11.9	12.0-12.4	12.5-12.9	13.0-13.4	13.5-13.9	14.0-14.9

Cells #634-#660, 30 Total

FIGURE 16. EVALUATION OF NORMALCY OF PERFORMANCE DATA

4. Conclusions

It has been successfully demonstrated that p-on-n silicon solar cells containing a lithium concentration of 1 to 5 x 10^{17}/cc in the base region recover from the degradation effects of high energy electron irradiation. The amount of, and period required for recovery, are dependent on the amount and rate of irradiation.

Considerably more evaluation of this type of cell must be made prior to classifying it as a truly operational device. Interaction of processing variables and materials require further investigation to establish the effects of actual lithium concentration with dislocations, oxygen content, and other impurities. Performance under various storage and environmental conditions will have to be evaluated.

III. ALUMINUM ANTIMONIDE

A. Introduction

From the standpoint of theoretical efficiency under the solar spectrum, aluminum antimonide, which has an energy gap of 1.6 ev, is considered a near ideal solar cell base material. However, it readily reacts with moisture and oxygen, and is therefore one of the more difficult semiconductors to work with.

The development of aluminum antimonide solar cells was undertaken initially by RCA-Mountaintop, under NASA Contract NAS5-3686, 1964-1965. Various p/n and n/p junction diffusion methods and contact materials were investigated. Results showed that the large area junctions which are required for solar cells could be achieved by impurity diffusion methods. Open-circuit voltages as high as 0.7 volts were achieved; however, cell efficiencies were less than one per cent, air mass one. A characteristic "S" pattern was continuously encountered in the photovoltaic V-I curves, as illustrated in Figure 17.

Since electron bombardment of AlSb effectively introduces donors, the work in the present program, NAS5-9576, has been concentrated on the p-on-n type cell. Cell characteristics were improved through refinements in diffusion and the development of a low resistance n-surface contact. Cell efficiencies have not appreciably improved. The limiting factor is that the zinc and cadmium used as the p-type diffusants characteristically form junctions about 5 mils deep. It has been concluded that this is too deep for efficient conversion of solar radiation, especially since no appreciable current generation has been observed

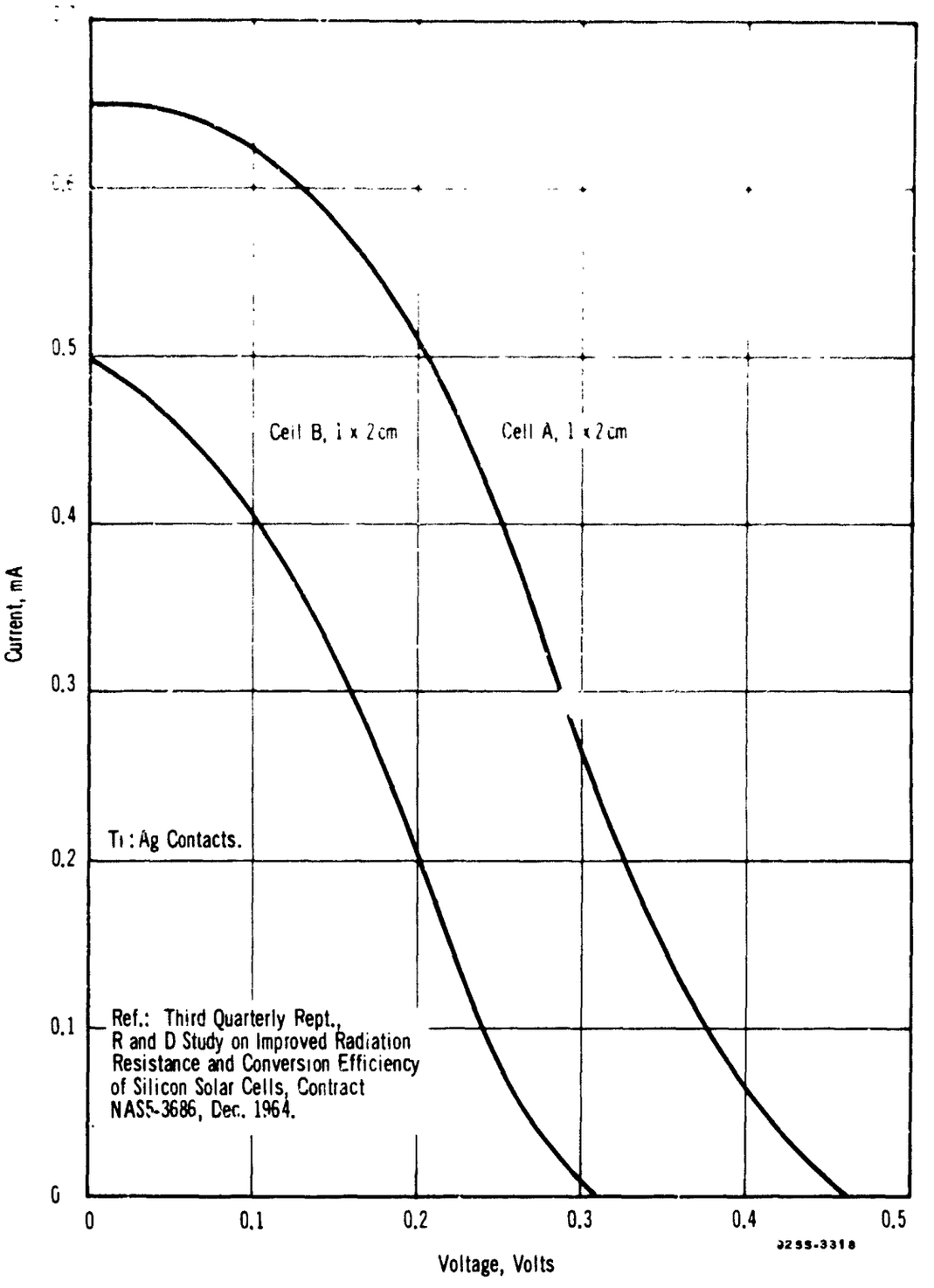

FIGURE 17. VOLTAGE-CURRENT CHARACTERISTICS OF ALUMINUM ANTIMONIDE, P-ON-N PROTOTYPE SOLAR CELLS

to occur in the front wall region of the cells. Details of the procedures and materials evaluated, and improvements in cell characteristics, are summarized in the following sections according to

1. Cell Design
2. Process Development
3. Solar Cell Performance

B. Cell Design

The mobilities of the current carriers are of the order of 40 to 200 $cm^2/(sec\text{-}volt)$ for aluminum antimonide. Also, the lifetimes of minority carriers are very low, of the order of 1 to 0.1 microseconds or less. These factors severely limit the volume of the aluminum antimonide which can effectively convert the solar radiation.

Figure 18 gives the distance in AlSb for 99% attenuation of incident radiation for wavelengths in the region 0.4 to 0.8 microns. The currents to be expected at given wavelengths of equal energy (Reference 8) are represented in Figure 19. From Figure 19, on a qualitative basis, the optimum junction depth is about 2 to 5 microns, provided current collection is realized within a distance of about 10 microns beyond the junction and 1.5 to 4 microns from the region between the junction and front surface. If no current collection occurs from the optical absorption in the front wall region, then a junction about 1 micron deep, with a diffusion length of about 10 microns, would convert a relatively large fraction of the incident energy.

The actual location of the junction can be estimated from the short-wavelength constant energy spectral response by the procedures

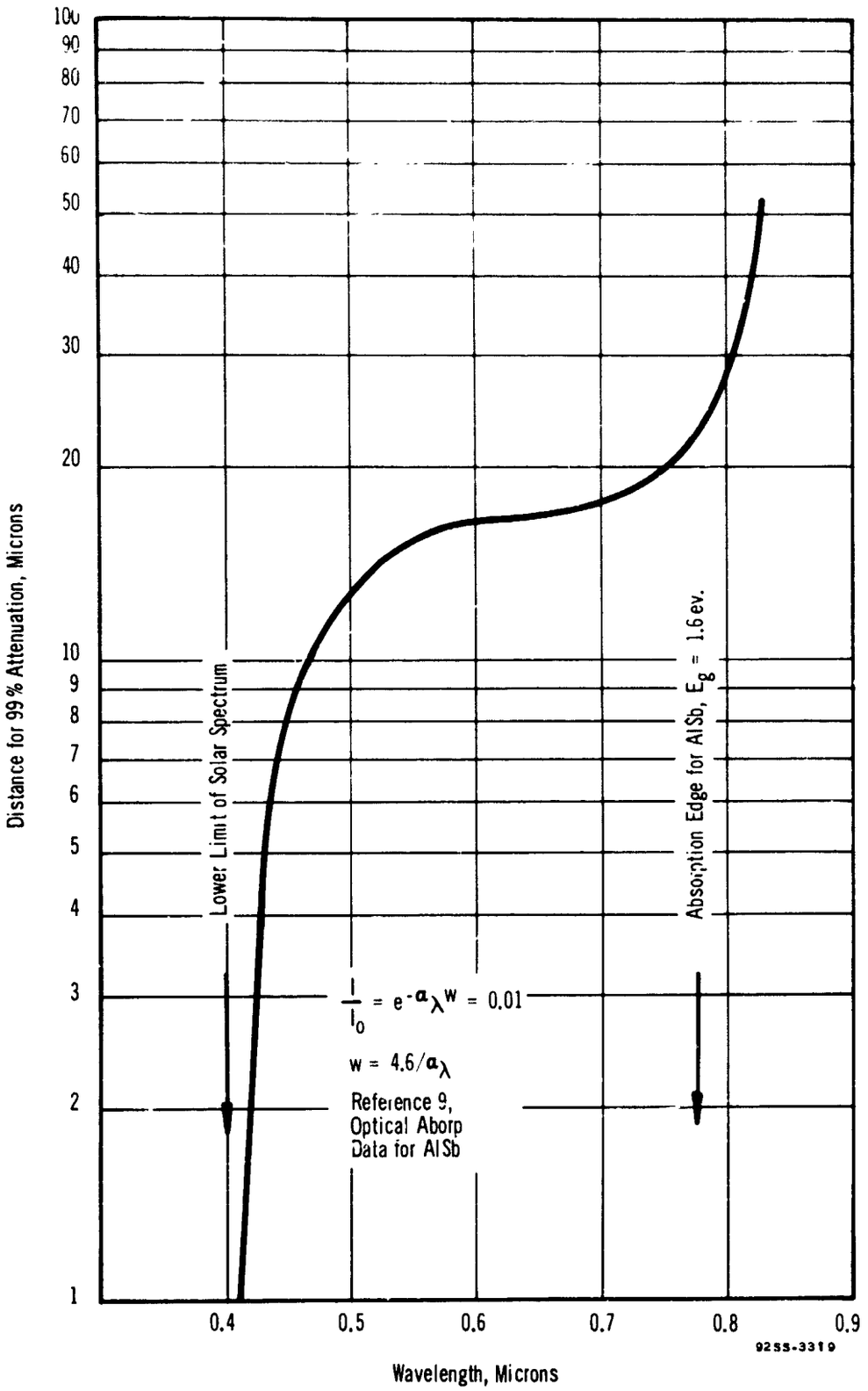

FIGURE 18. ABSORPTION DISTANCE VERSUS WAVELENGTH IN ALUMINUM ANTIMONIDE

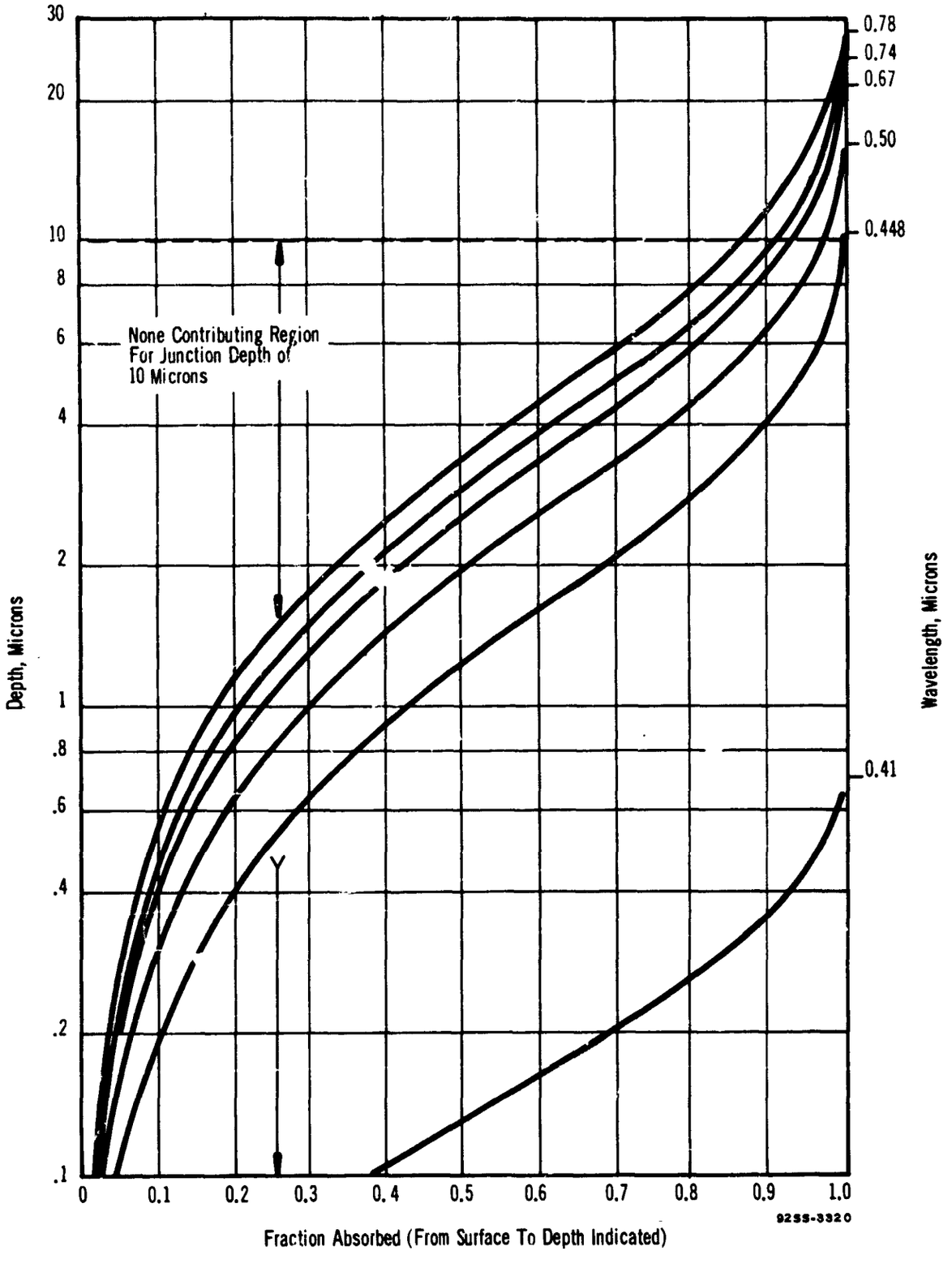

FIGURE 19. SPECIAL DISTRIBUTION OF OPTICAL ABSORPTION IN ALUMINUM ANTIMONIDE

outlined in Appendix I of Reference 8. Figure 20 gives the junction depth in terms of the short-circuit current ratios at the wavelengths 0.5 and 0.44 microns. This has served as a non-destructive means of measuring junction depths in the various diffusion tests described under the section "Diffused Junctions in Aluminum Antimonide".

C. Processing Development

The following sections describe the progress in the various phases of process development, including:

1. Pre-Diffusion Surface Preparation.
2. Diffusion Procedure and Determination of Zinc Diffusion Constant.
3. Contacts.
4. Post Diffusion Surface Etch and Effect on V-I Characteristics and Spectral Response.

1. Pre-Diffusion Surface Preparation

Aluminum antimonide when exposed to air develops a highly resistive surface, consisting of aluminum and antimony oxides. Various surface treatments have been evaluated in Reference 10 to eliminate these oxides. The etchants were

HNO_3 with formic acid, in various ratios,

HNO_3 with H_2SO_4, and H_2O_2 with HF.

Five parts H_2O_2 with one part HF gives a bright smooth surface similar to that achieved for Si and GaAs.

2. Diffusion Procedures and Results

Diffusion Procedure

The closed-box system for diffusion of zinc, similar to that used for gallium arsenide solar cells, and used in the NAS5-3686 program, continued to be satisfactory. Diffusion temperatures were from 600 to 750°C. Times of 2 to 25 minutes were evaluated.

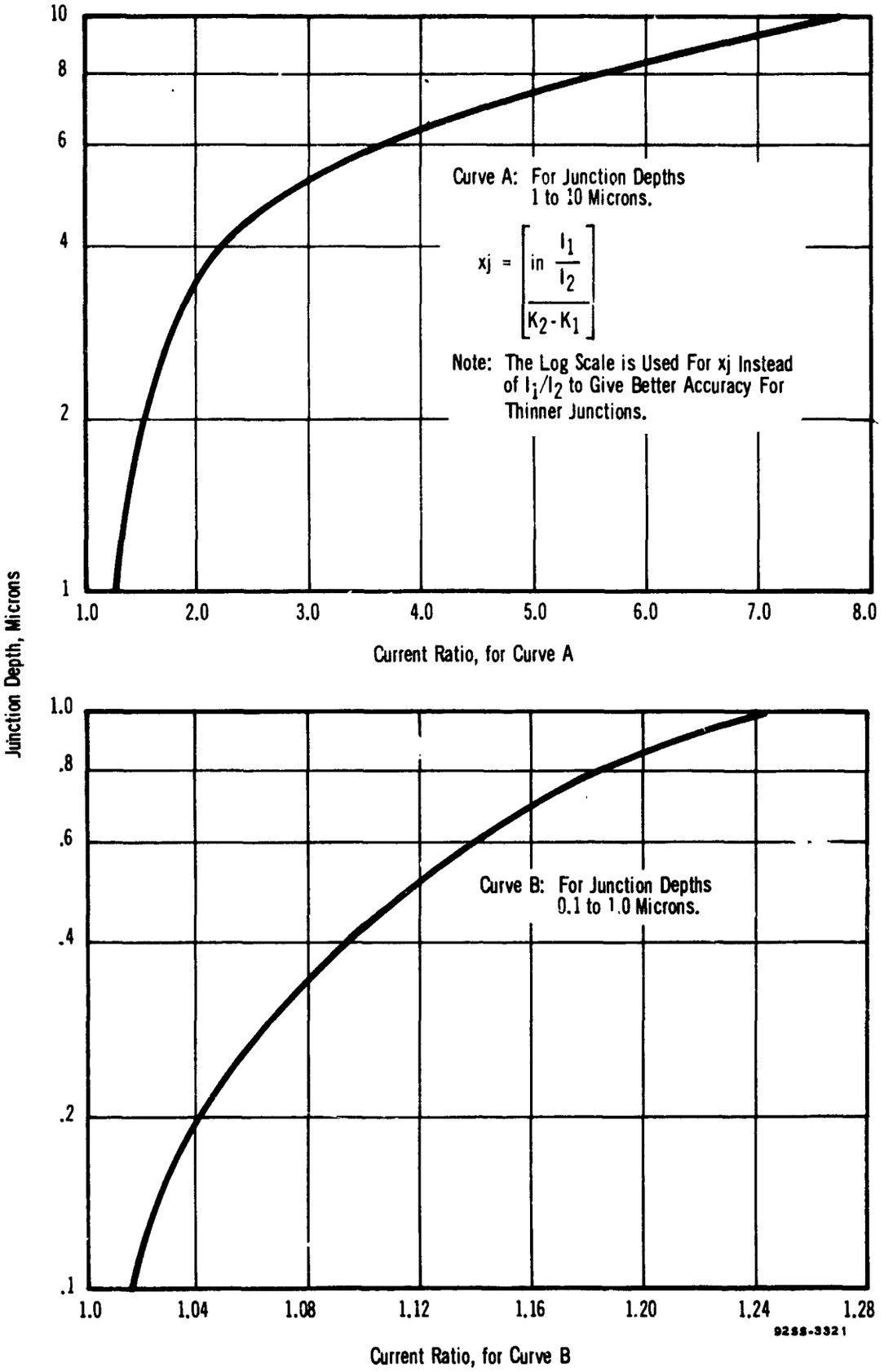

FIGURE 20. ALUMINUM ANTIMONIDE THEORETICAL SHORT-CIRCUIT CURRENT RATIO FOR THE 0.500 MICRON AND 0.448 MICRON WAVELENGTH BANDS VERSUS JUNCTION DEPTH

Characteristics of Zinc Diffused Junctions in Aluminum Antimonide

The junction depths achieved for practical ranges of diffusion time and temperature are shown in Figure 21. The zinc diffusion is accomplished using the closed box diffusion method described in Reference 11. The open-circuit voltages as indicated show that below diffusion temperatures of about 650°C and for diffusion times of less than about 3 minutes at temperatures up to about 800°C, the 0.7 to 0.8 volts capability of aluminum antimonide is not realized. Temperatures above 800°C are not practical due to the onset of thermal decomposition of the aluminum antimonide. In between these limits, the junction depths are greater than 5 microns, which since there is little collection from the front wall of the device, restricts the efficiency of the cell. Most of the incident radiation of the spectral region of interest, 0.4 to 0.8 microns, is absorbed within about 10 to 15 microns of the front surface (see Reference 8). With little energy conversion arising from the front wall region, and only a fraction available from absorption in the region beyond the junction, the efficiencies would be expected to be severely limited. For this type of cell, etching of the front surface to reduce junction depths has not been satisfactory due to the appreciable reduction in open-circuit voltage.

Characteristics of Cadmium Diffused Junctions in Aluminum Antimonide

Figure 22 presents the approximate junction depth obtained by diffusing cadmium into aluminum antimonide at various times and temperatures. The results are similar in treatment to those obtained for zinc. Below 700°C the solubility is insufficient to yield

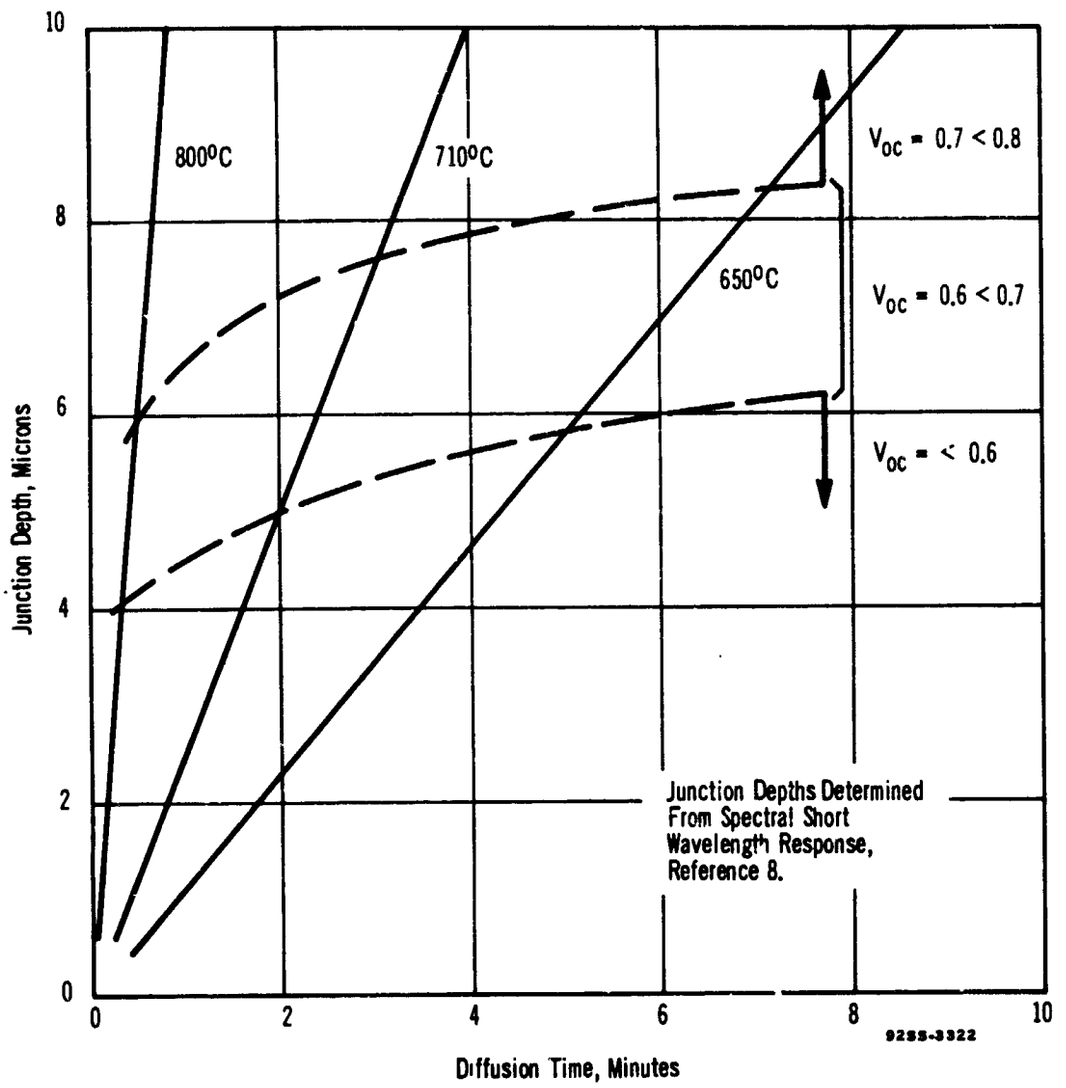

FIGURE 21. DIFFUSION CHARACTERISTICS OF ZINC IN ALUMINUM ANTIMONIDE

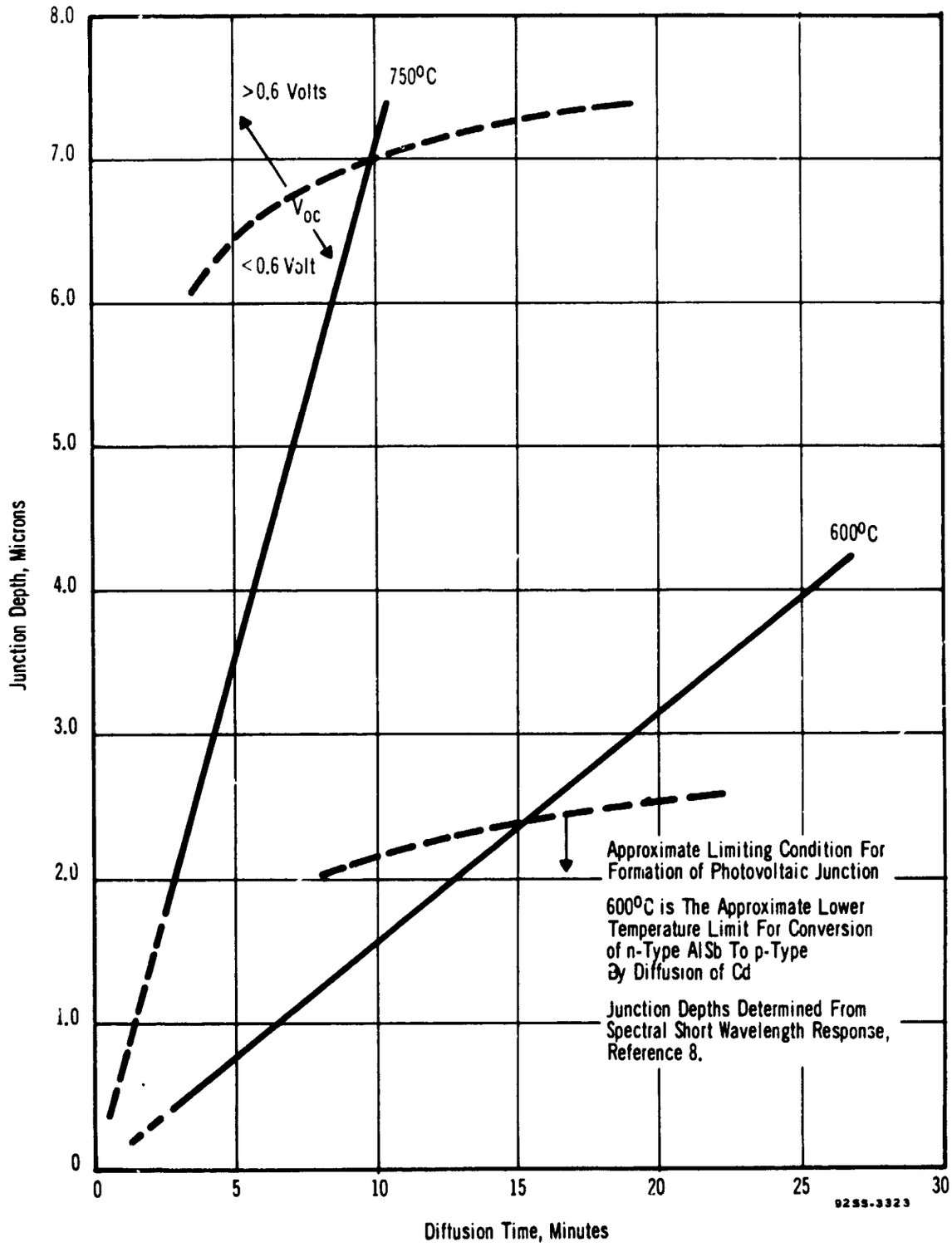

FIGURE 22. DIFFUSION CHARACTERISTICS OF CADMIUM IN ALUMINUM ANTIMONIDE

satisfactory open-circuit voltages. For higher temperatures, diffusion times above about 5 minutes are required to give satisfactory voltages. For these conditions, the junctions are too deep to yield high efficiency cells.

3. Contacts

The various elements and compounds evaluated as contact materials were as follows:

Zn:In (Good physical contact to p layer, but indication of shorting through the junction).

Pb (Ultrasonically soldered), good ohmic contact to n-type).

Ce (Acts as p-type dopant).

Li (High resistance on n-type).

In (Acted as p-type dopant, high resistance).

Ti:Ag (Non-ohmic to n and p AlSb).

Ag Epoxy, Ag Evaporated (Non-ohmic to n and p AlSb).

The results were that Ce is very reactive in air at medium temperatures, 300°C, to produce decided p-type doping. The In and Li were ineffective as either ohmic contacts or as dopants. The Pb, especially when ultrasonically soldered, considerably reduced the resistance of the contact to n-type aluminum antimonide.

Of particular note was the success of Pb to eliminate the apparent double junction effect in the photovoltaic V-I characteristic, as noted in Figure 23.

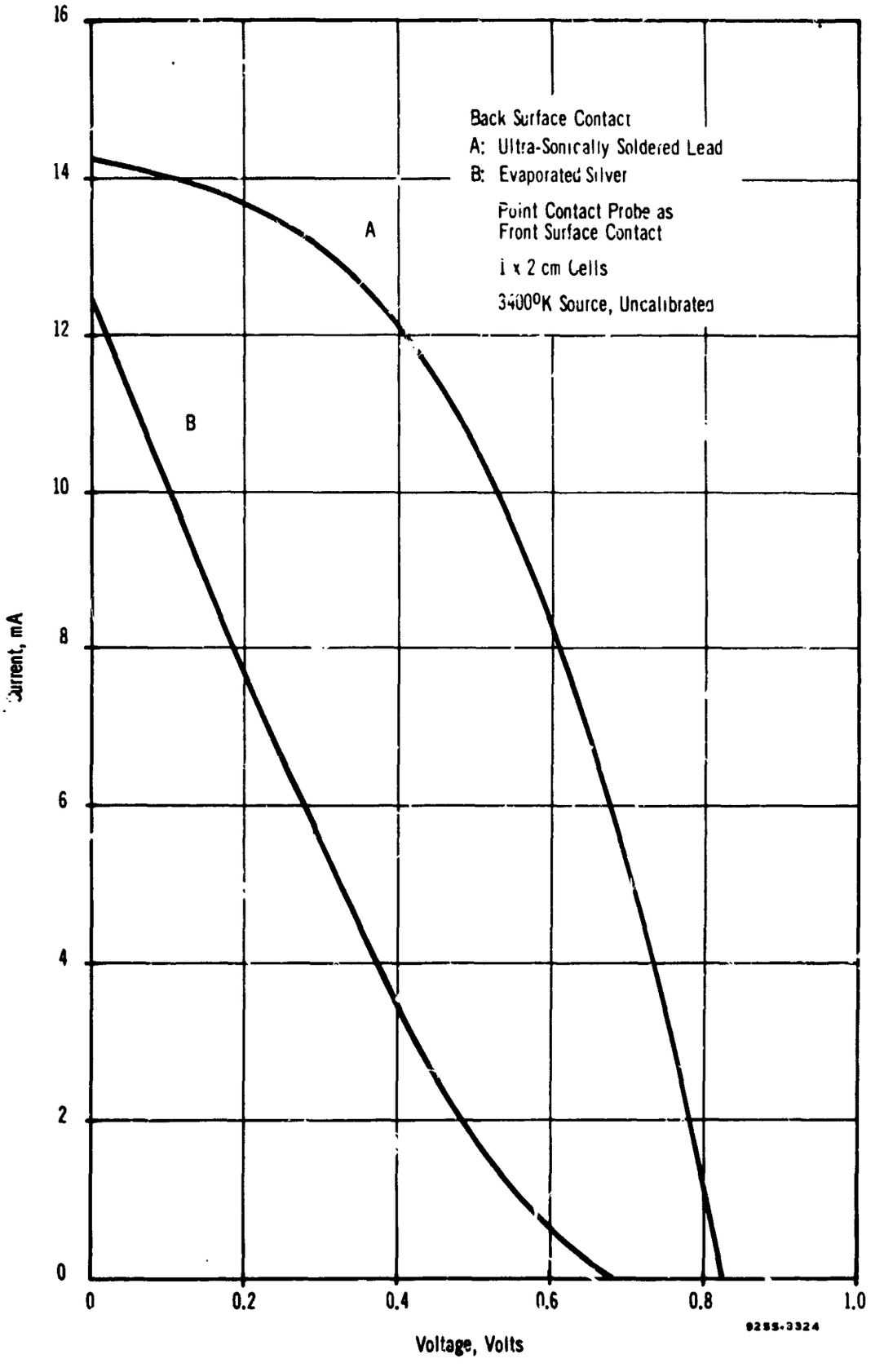

FIGURE 23. EFFECT OF LEAD AS CONTACT TO N-TYPE ALUMINUM ANTIMONIDE BASE

4. Post Diffusion Surface Etching, Effect on V-I Characteristic and Spectral Response

A post diffusion surface etch consisting of immersion in five parts H_2O_2 and one part HF, successively for 3 to 4 seconds was used to remove surface films and to generally improve the short-circuit current output of the cells. The effect of repeated etching is given in Figures 24 and 25, showing the changes in respectively the V-I and the spectral response characteristics.

D. Cell Performance and Diode Characteristics

The aluminum antimonide principally used consisted of (100) orientated wafers from the two crystals (Bell and Howell) listed below:

AlSb Crystals Used in P-on-N Cells

Bell and Howell Crystal No.	Orientation	Carrier Density	Mobility	Resistivity
		atoms/cm^3	cm^2/volt-sec.	ohm cm
79	(100)	1.22×10^{17}	175	0.294
67	(100)	1.01×10^{17}	165	0.374

The primary means of evaluating cell performance has been the photovoltaic V-I characteristic under several conditions.

For quantitative measurements, 2800°K, 3400°K and 5800°K sources, calibrated for 100 mw, were used.

The V-I curves for various Zn and Cd diffused cells are illustrated in Figures 26, 27, and 28. It is seen that the general

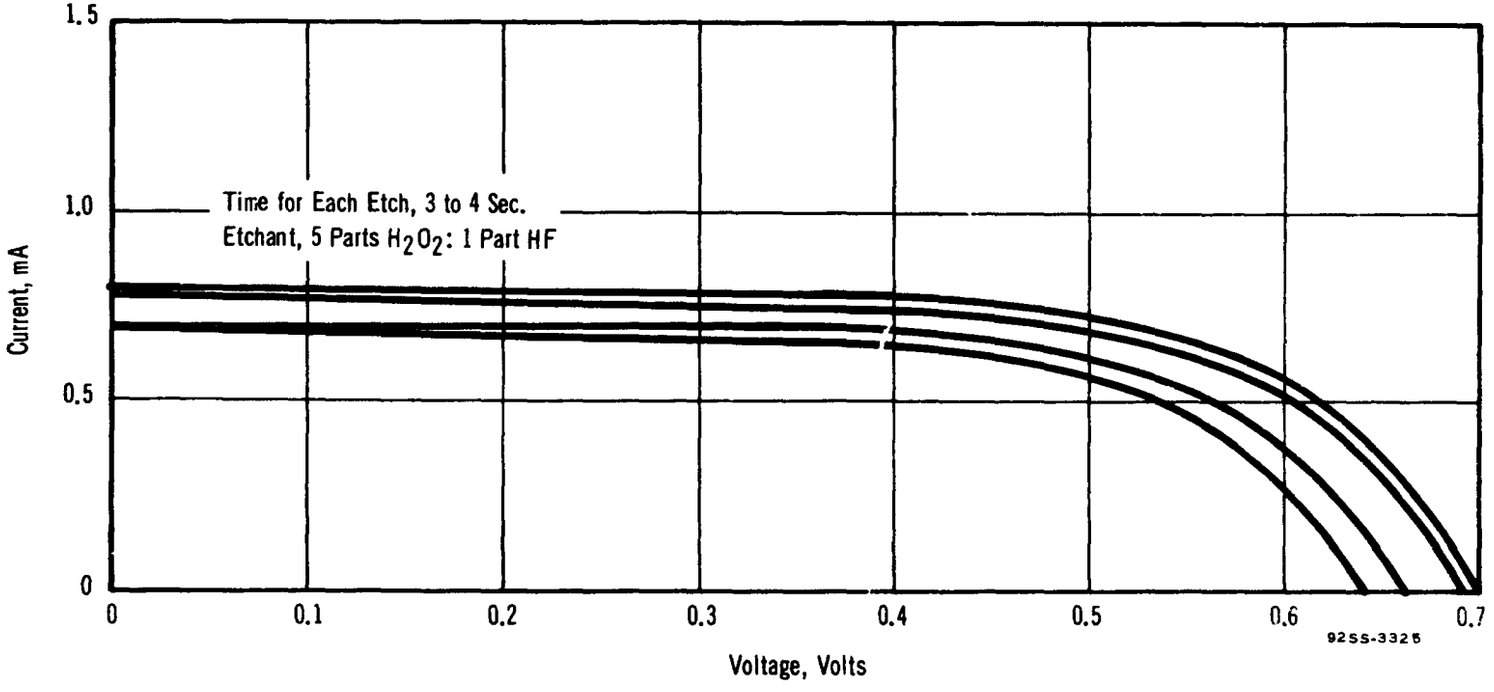

FIGURE 24. EFFECT OF REPEATED SURFACE ETCHING ON VOLTAGE-CURRENT CHARACTERISTICS

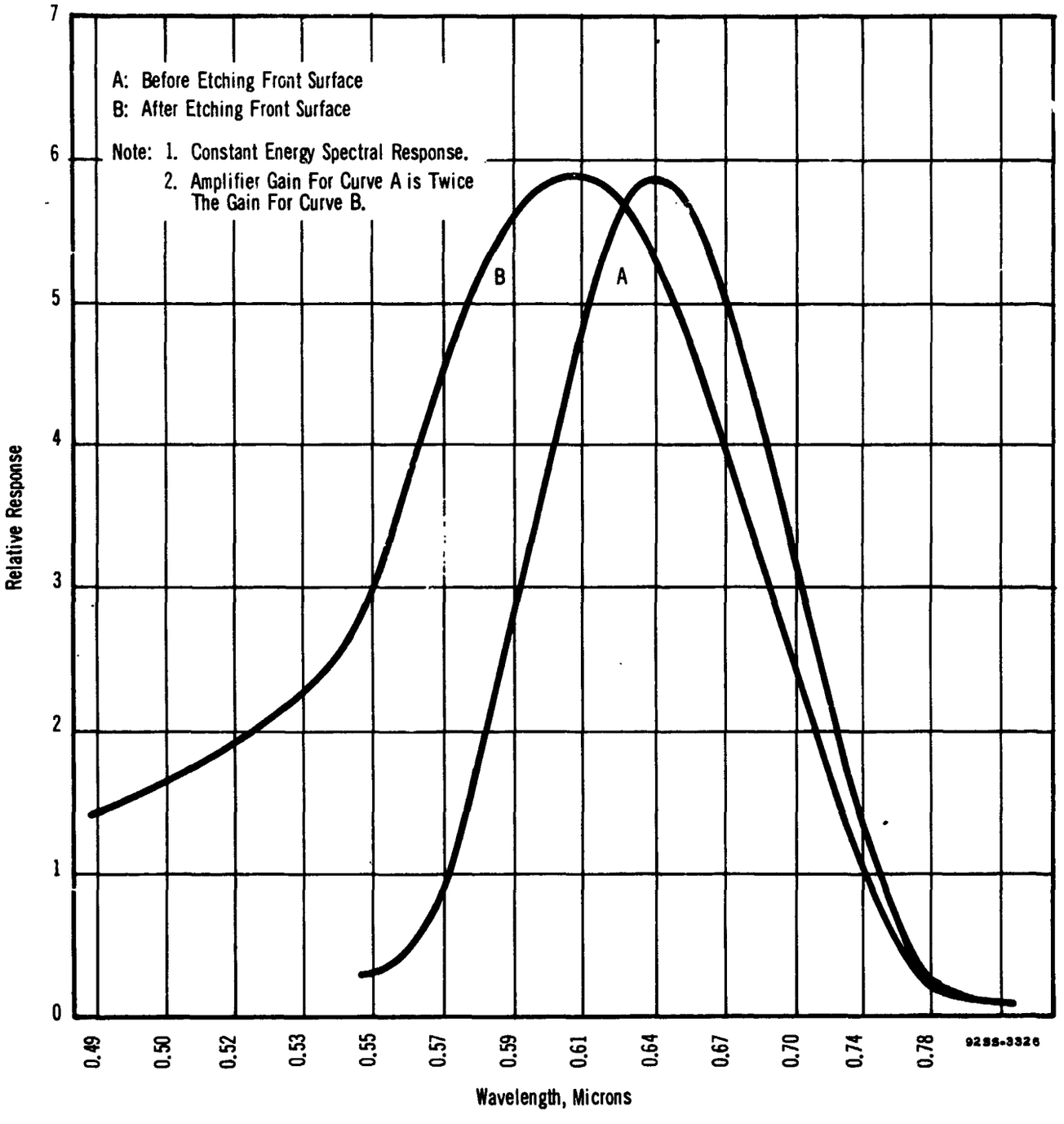

FIGURE 25. SPECTRAL RESPONSE OF ALUMINUM ANTIMONIDE SOLAR CELL AND EFFECT OF SURFACE ETCHING ON SPECTRAL RESPONSE

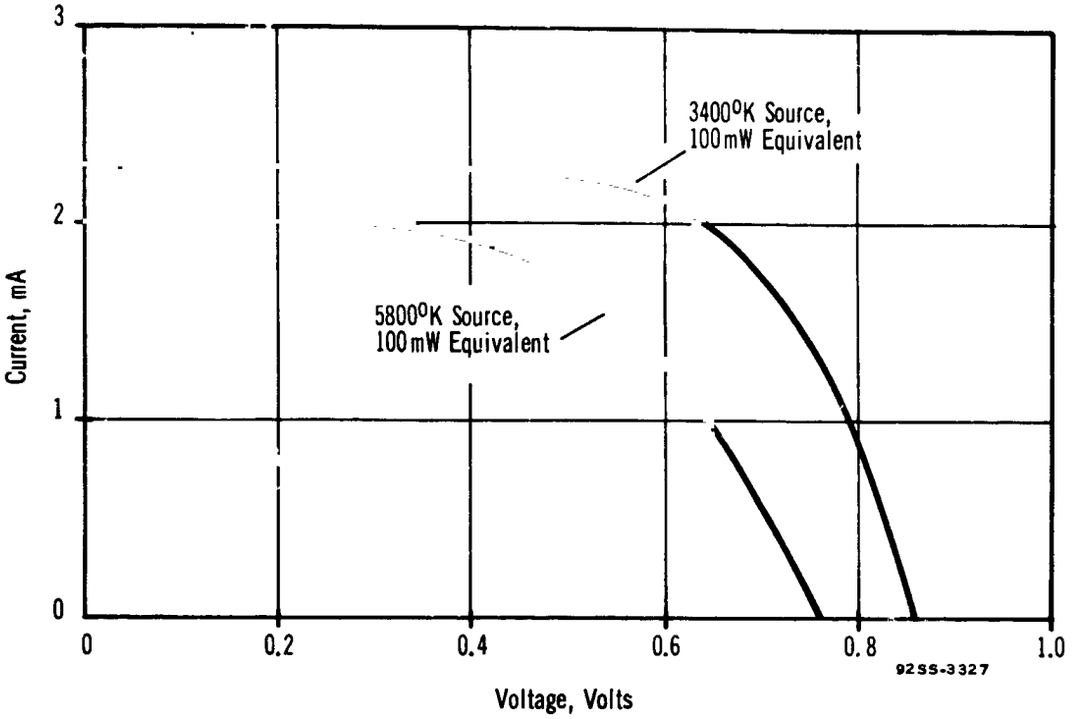

FIGURE 26. TYPICAL ZINC DIFFUSED AlSb CELL VOLTAGE-CURRENT CURVES FOR 100 mW, 3400°K AND 5800°K SOURCES

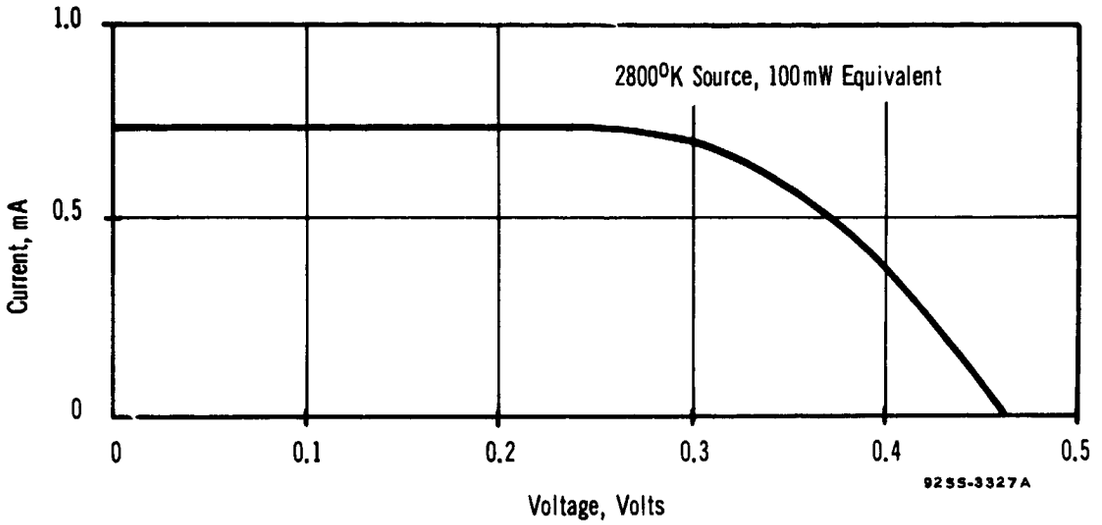

FIGURE 27. TYPICAL ZINC DIFFUSED AlSb CELL VOLTAGE-CURRENT CURVES FOR 100 mW, 2800°K SOURCE

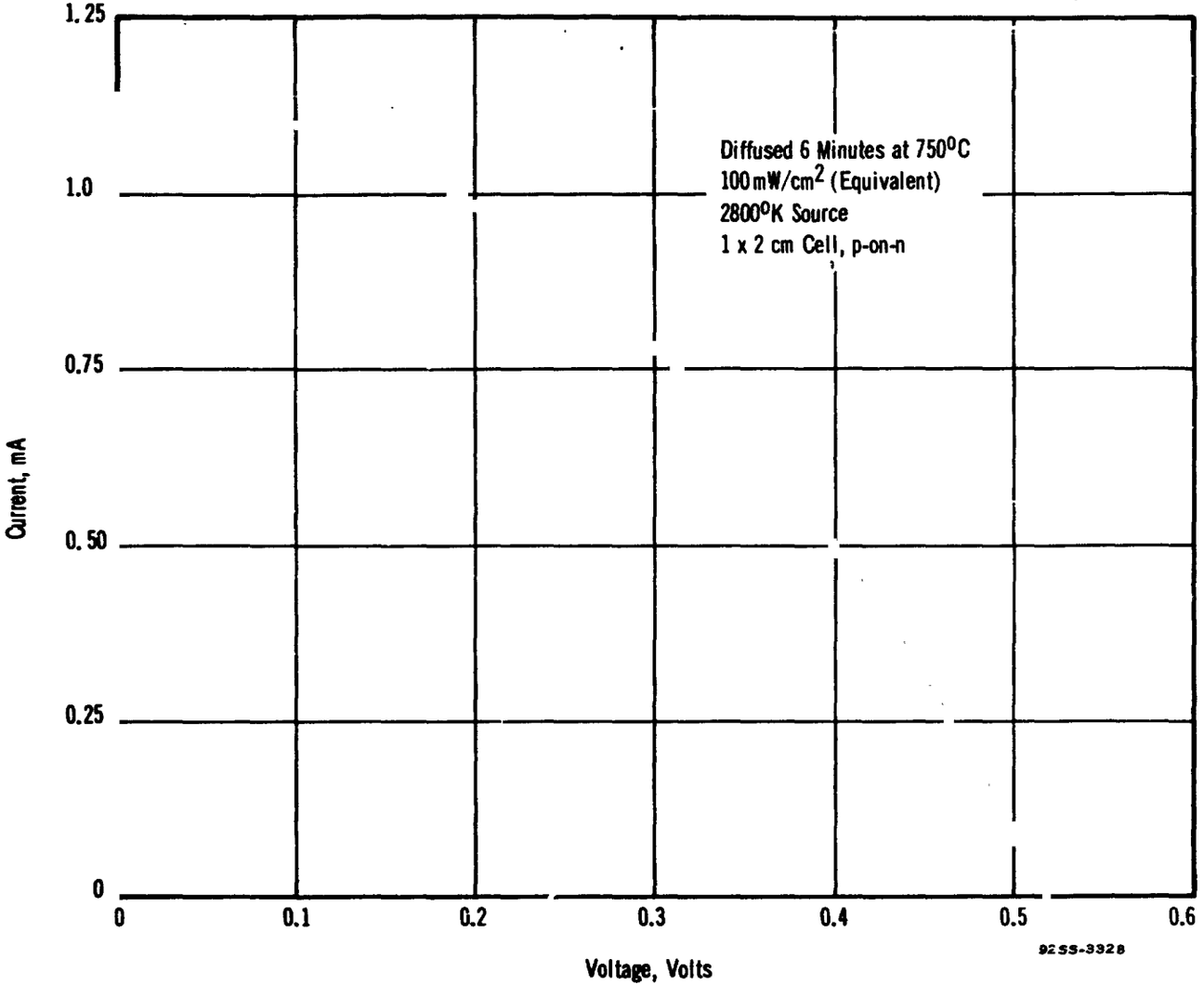

FIGURE 28. VOLTAGE-CURRENT CURVE REPRESENTATIVE OF CADMIUM-DIFFUSED ALUMINUM ANTIMONIDE SOLAR CELL

shape conforms to the idealized photovoltaic equation, namely

$$I = I_L - I_o (e^{qV/nkT} - 1)$$

Very low I_{sc} is explained on the basis that the junctions are too deep and the diffusion length of carriers too short for optimum energy conversion of the 0.4 to 0.8 spectrum.

Diode Characteristics, Determination of Basic Parameters

The general form of the photovoltaic diode equation is

$$I = I_L - I_o (e^{q(V-IR)/nkT} - 1) = I_L - I_o (e^{qV/nkT} - 1)$$

where the terms have their usual significance.

I_o - is the reverse saturation current.

I_L - is the generated current.

V - is the applied voltage.

n - is an empirical factor proportional to the recombination currents in the junction.

q - is the electron charge.

k - is Boltzman's constant.

T - is the temperature, degrees Kelvin.

R - is the series resistance.

For low values of I, the series resistance tern can be neglected. The two boundary conditions,

$$V = V_{oc} \text{ for } I = o$$

and

$$I = I_{sc} \text{ for } V = o$$

defines the various parameters. Thus, for the case of no illumination,

$$I_L = o$$

otherwise

$$I_L = I_{sc}$$

The individual parameters are therefore given by

$V_{oc} = (n/38.6)\ \mathrm{In}\ (I_{sc}/I_o + 1)$

$I_{sc} = I_o\ (e^{38.6\ V_{oc}/n} - 1)$

$I_o = I_{sc}/(e\ 38.6\ V_{oc}/n - 1)$

$n = 38.6V/\mathrm{In}(I/I_o + 1)$ or $38.6V/\mathrm{In}\ I_1(I_2-I_1)$

where

38.6 - is the value of q/kT at room temperature

and

V_1 - is an arbitrary low voltage sufficient that I_1R is negligible in comparison, non-illuminated case.

I_1 - corresponds to V_1.

I_2 - corresponds to V_2, for which I_2R is still negligible compared to V_2 and $V_2 = 2\ V_1$.

The results of analyzing the dark and illuminated V-I characteristics of the AlSb cell shown in Figures 29 and 30 were

for $V_{oc} = 0.62$ volts, $I_{sc} = I_L = 0.5 \times 10^{-3}$a

$I_o = 0.13 \times 10^{-6}$ a.

$n = 6.6$

Substitution of these values in the original diode equation, and plotting I versus V gives a reasonable regeneration of the illuminated V-I characteristic, as shown in Figure 29.

It is concluded since I_o is reasonably small, that the junction approximates that of a good diode. On the other hand, the n value of 6.6 is high compared to GaAs, 2 to 3, and indicates a high level of recombination of carriers occurring within or near the junction.

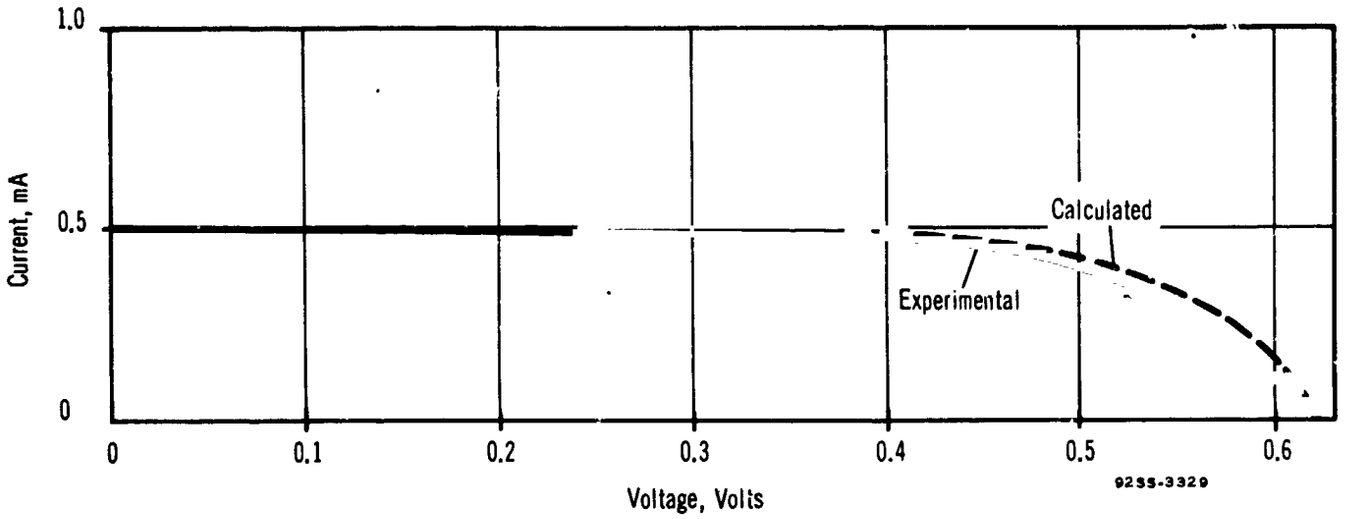

FIGURE 29. PHOTOVOLTAIC V-I CURVE AND CALCULATED CURVE BASED ON NON-ILLUMINATED DIODE CHARACTERISTICS

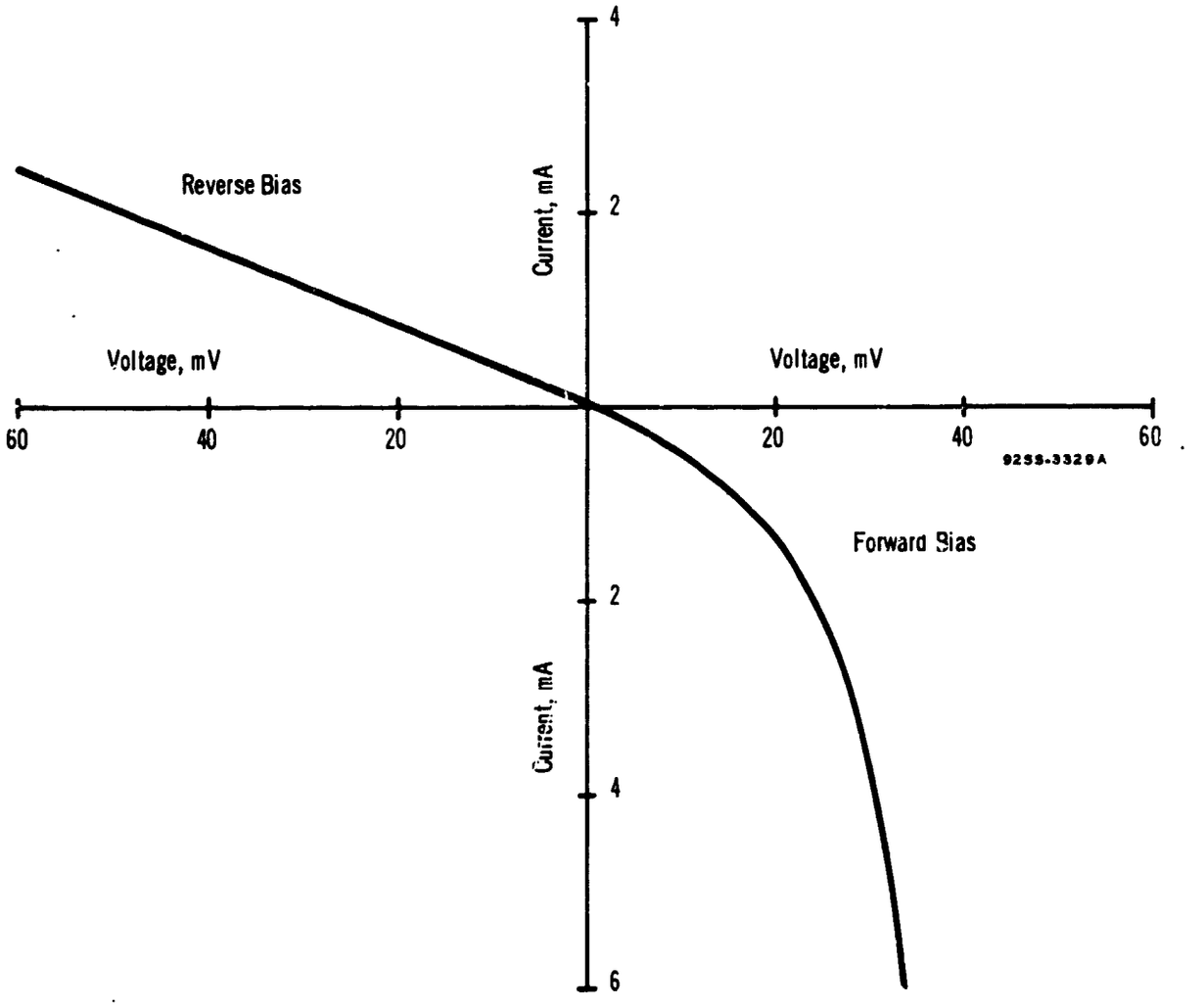

FIGURE 30. NON-ILLUMINATED V-I CHARACTERISTICS

E. Spectral Response

The spectral response curves for typical aluminum antimonide cells are given in Figures 25 and 31. The wavelengths of peak response and half maximum amplitude (absorption edge) as a function of the diffusion time is given in Figure 32. The absorption edge of AlSb is 0.78 microns. From the spectral response, the values range from 0.59 to 0.72 microns, as included in Figure 32. Decrease of the red response associated with increasing diffusion times, except for the 20 minute region, is explained on the basis that the deeper junctions actually approach the depth corresponding to the absorption edge of aluminum antimonide, about 10 microns. As this limit is reached, proportionately less current is collected from the back-wall region than from the front-wall region of the cell. The shift of the peak response wavelength to shorter wavelengths as the diffusion time is decreased is explainable on the basis of the very short lifetimes encountered in aluminum antimonide. For the shorter diffusion times, carriers generated in the bulk, corresponding to the long wavelengths, have such a short diffusion length, that they simply do not reach the shallow junctions to contribute to the current.

F. Radiation Effects and Environmental Tests

Radiation Effects

The end result of irradiation for pertinent solar cell materials is:

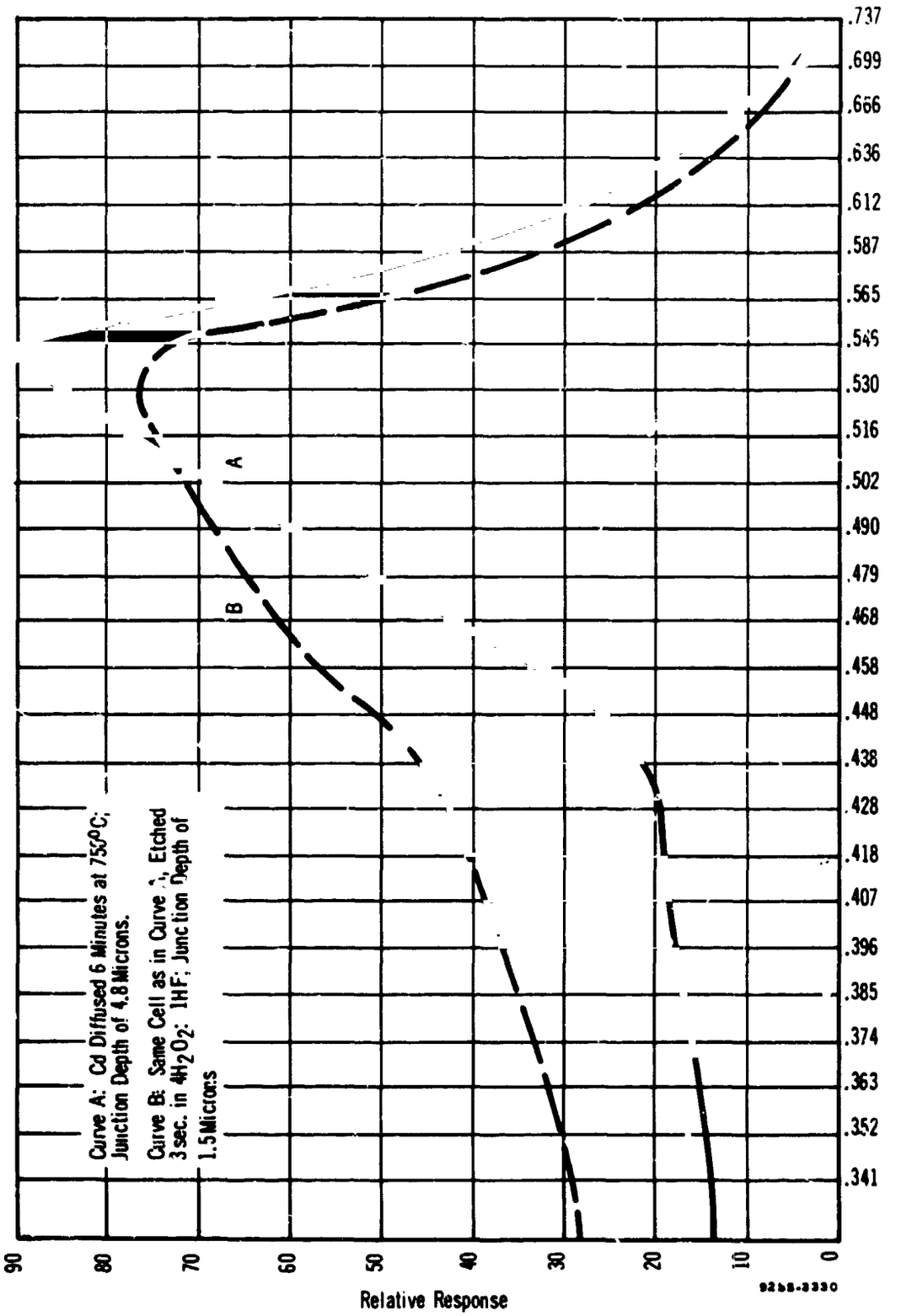

FIGURE 31. SPECTRAL RESPONSE OF CADMIUM-DIFFUSED ALUMINUM ANTIMONIDE SOLAR CELL

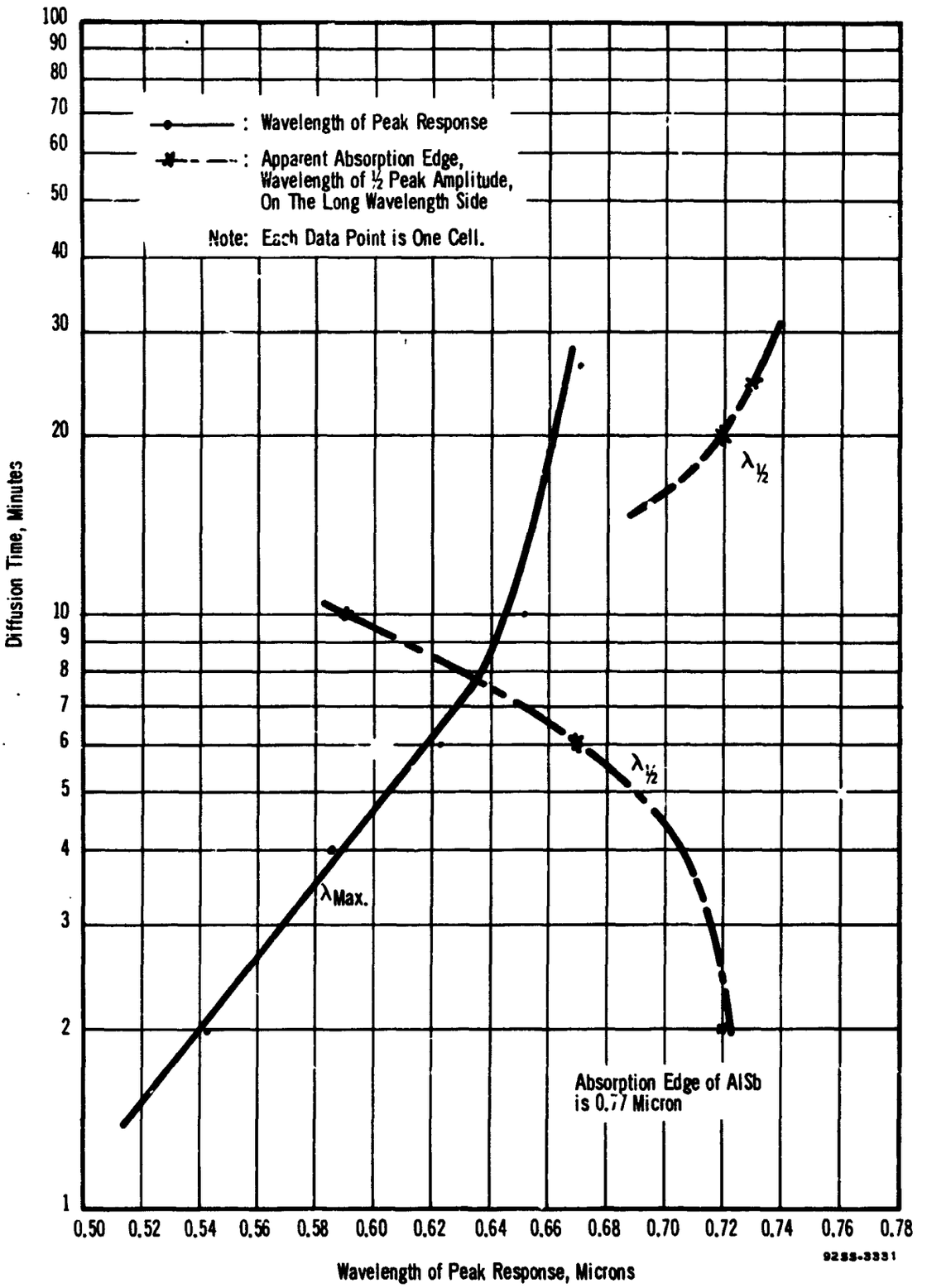

FIGURE 32. EFFECT OF DIFFUSION TIME ON WAVELENGTH OF PEAK RESPONSE AND APPARENT ABSORPTION EDGE

Material	End Result of Irradiation	Reference
Si	becomes intrinsic	13
AlSb	becomes n-type	13
GaAs	becomes intrinsic	14

The choice of n-type AlSb as the base material therefore minimizes the probability that the radiation introduced defects, effectively donors, will appreciably affect the over-all cell performance.

Since cell efficiencies to date have been less than 3%, irradiation tests of state-of-the-art cells have not been made.

Environmental Tests

Qualitatively it has been observed that severe problems exist in two specific areas; junction edges, and the junction proper. To obtain reliable readings on cell performance, the cells must be edge cleaned prior to testing, especially if an elapsed time of more than 4 hours has occurred since the last edge cleaning. Surface oxidation is of course expected. Over a period of 48 hours, it has also been observed on occasions that a junction previously capable of an open-circuit voltage of 0.76 volt decays to about 0.4 volt, even when stored in a desiccator and the edge cleaning is repeated. These effects emphasize the importance of developing a surface passivating coating.

G. Conclusions

Aluminum antimonide continues to show promise as an optimum solar cell material. The spectral response of prototype solar cells has closely matched the solar spectrum. Cells having 1%

efficiency, air mass one, have been achieved. These cells are lacking in suitable front surface contacts and do not have optical anti-reflective coatings. Developments in both areas will certainly further improve this type solar cell.

The main factors limiting the performance of the cells to about 1% efficiency is the deep junctions characteristically formed by the diffusants zinc and cadmium. The requirement is therefore a sufficiently soluble slow diffusing dopant, a unique diffusion technique, or a combination diffusion-surface etch method.

IV. MISCELLANEOUS DEVELOPMENTS

Thermal Annealing To Improve Carrier Lifetime

The severe degradation of minority carrier lifetimes during the processing of solar cells and lack of significant effect on performance has been noted in a previous development program, NAS5-457, Reference 12, "Radiation Damage to Silicon". The lifetime of minority carriers as measured in completed cells is nearly independent of the lifetime observed in the starting material. For example, both 200 and 900 microseconds for the initial material deteriorated to 10 to 15 microseconds for typical 10 ohm cm n-on-p silicon solar cells. The relative effects of both the diffusion and contact sintering cycles on minority carrier lifetime have been determined in the present program, as illustrated in Table III. In Column 1, a bar of silicon, 0.25 x 0.25 x 0.875 inch, was degraded from an initial 200 microseconds lifetime to 10 microseconds by the 875°C - 25 minute diffusion thermal cycle. (No diffusant was present in the diffusion tube.) Column 2 shows that a slow cool from 200°C to room temperature improves the final lifetime only slightly, to 14 microseconds. A thermal annealing cycle of 450°C for 5 hours restores the lifetime to 21 microseconds, Column 3. Increasing the annealing time to 20 hours did not increase the lifetime beyond the 21 microseconds. It is significant that the thermal cycle of 605°C for 5 minutes, conventionally used in sintering the Ti:Ag contacts, reduces the 21-microsecond bar to 14 microseconds, as illustrated in Column 5. A repetition of the sintering cycle, Column 6, shows that a second sintering cycle further reduces the carrier lifetime to 10 microseconds.

Two questions arise from this data on the recovery of minority carrier lifetime by thermal annealing. What is the effect on actual cells, and what would be the probable ultimate effect after irradiation if initially high lifetimes were possible? Two groups of twenty cells each were thermally annealed at 400°C for 5 hours. The power-output at 0.46 volts for both groups increased by at least 3.2% and as high as 12%. The changes noted for one group of 20 n-on-p production type cells are illustrated in Figure 33, before and after annealing, respectively.

The significance of increasing the initial lifetimes (diffusion lengths) on final performance under high energy irradiation can be estimated from the usual relations

$$(1/L_f^2) = (1/L_i^2) + K\,\phi$$

and

$$I_{sc} = A\,q\,g_o\,L_f$$

The carrier generation rate, g_o, as a result of the spacial distribution of optical absorption, is dependent on L_f. A qualitative prediction of the final performance of cells with initially long diffusion lengths can be made by calculating the final diffusion lengths as a function of irradiation dosage. Figure 34 shows the calculated final diffusion lengths as a function of irradiation for nominally 10 ohm cm p-type silicon, based on the assumption that the defect introduction rate K does not appreciably vary with either dosage or initial diffusion length. It is evident that for dosages up to about 10^{13} electrons per sq. cm, very high initial lifetime material would possibly exhibit some improvement in radiation resistance. However, at dosages above 10^{14} electrons per sq. cm, the difference between cells having 200 or 1000 microns initial diffusion lengths would be indistinguishable.

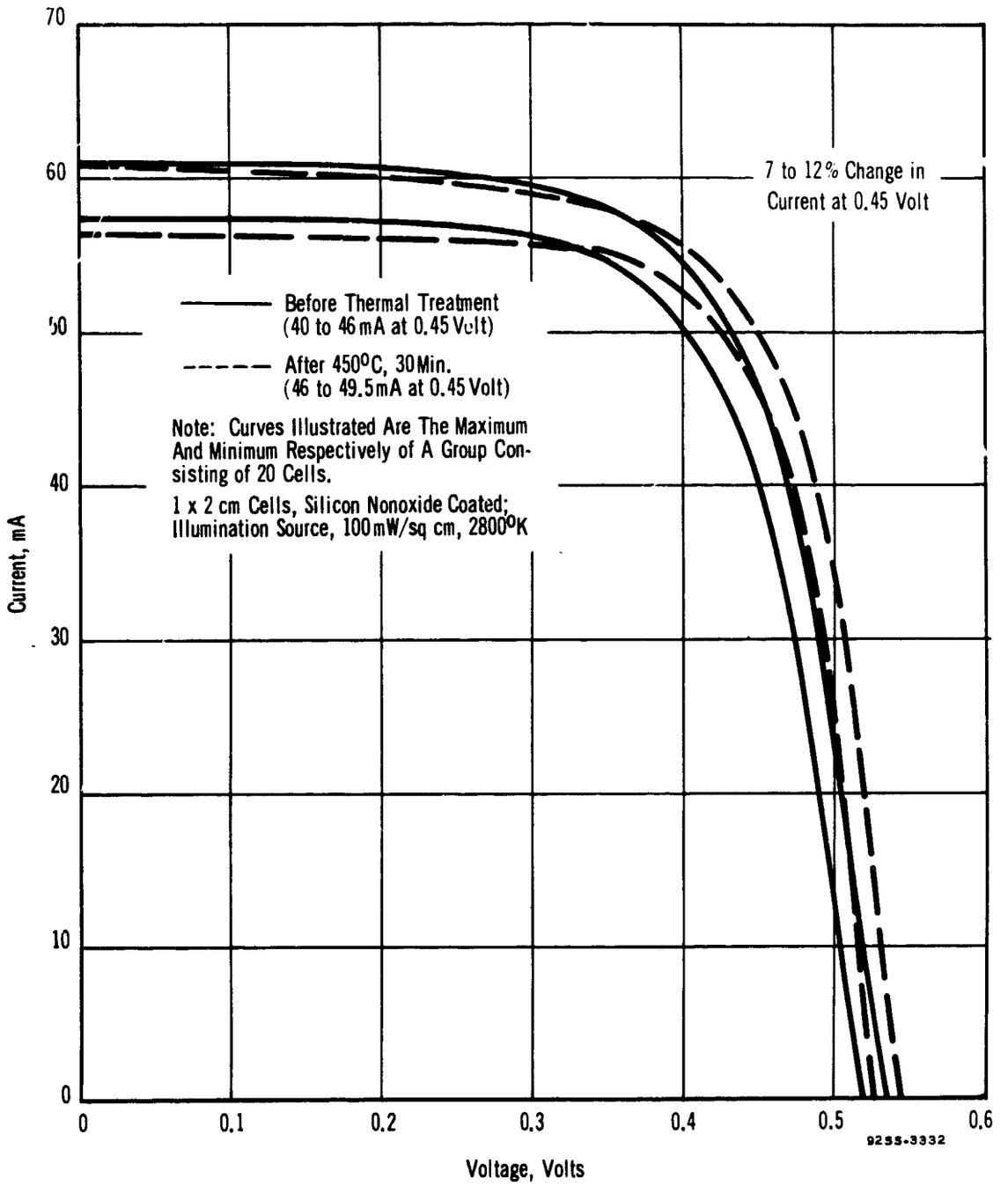

FIGURE 33. RANGE OF VOLTAGE-CURRENT CHARACTERISTICS OF 20 N-ON-P PRODUCTION CELLS BEFORE AND AFTER HEAT TREATMENT

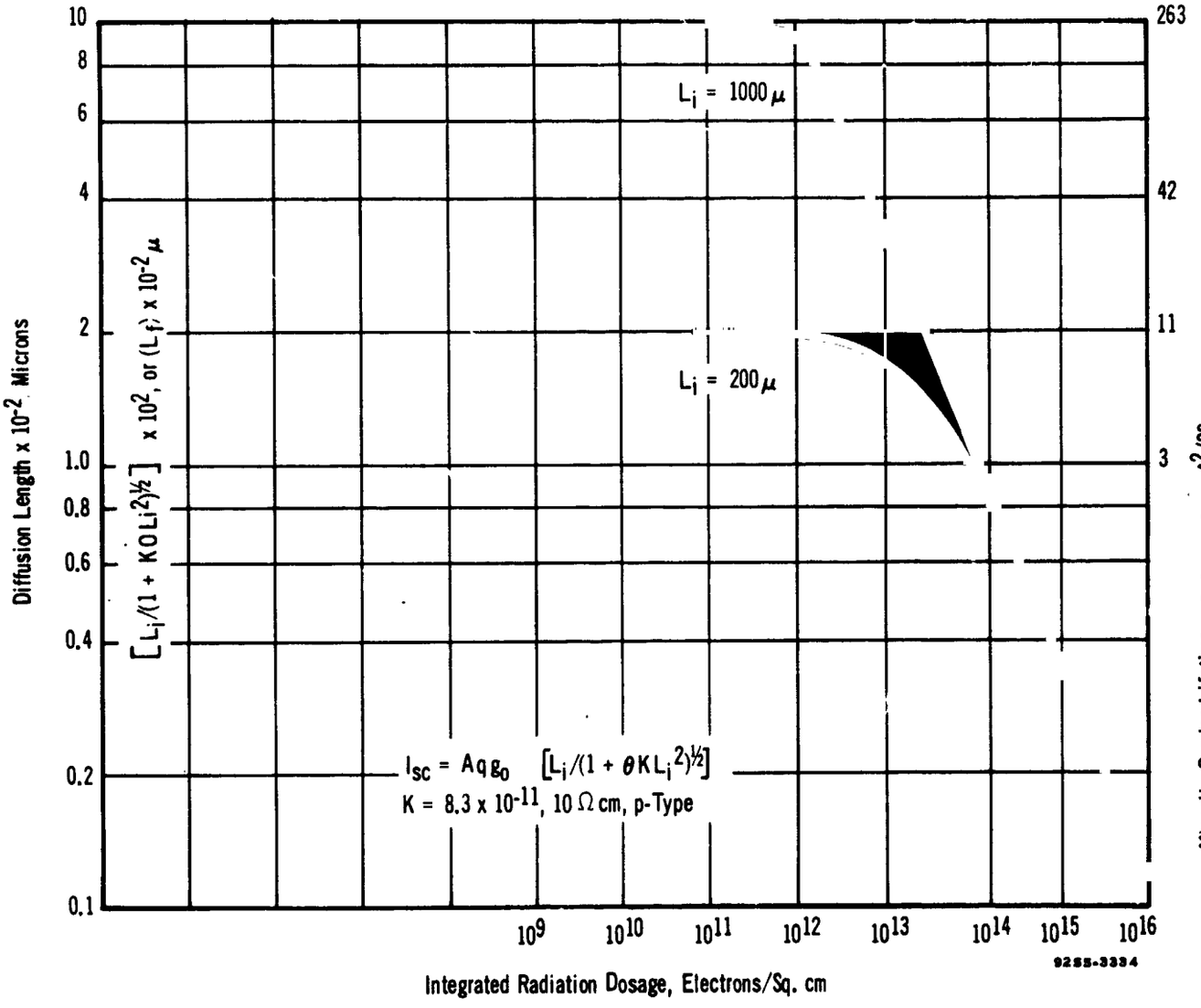

FIGURE 34. PREDICTED EFFECT OF 1 MeV ELECTRON IRRADIATION ON THE MINORITY CARRIER DIFFUSION LENGTH FOR VARIOUS INITIAL VALUES OF DIFFUSION LENGTH

It is concluded that even though increased initial efficiencies can be realized by thermal annealing procedures, the performance at irradiation dosages above 10^{14} electrons per sq. cm would not be improved. With respect to the lithium diffused cells, Section II, thermal annealing to achieve initially high diffusion lengths would not yield cells having as high a performance in high energy environments.

TABLE III

EFFECT OF VARIOUS THERMAL TREATMENTS ON MINORITY CARRIER LIFETIME

		1	2	3	4	5	6
Crystal Type		C					
Conductivity Type		p					
Initial Resistivity, ohm cm		34-38					
Initial Lifetime, microseconds		200					
Heat Cycle:	Temperature, °C	875	875			605	605
	Time, minutes	25	25			5	5
	Gas	N	N			H	H
Quench:	High Temperature, °C	875	875			605	605
	Final Temperature, °C	27	200			27	27
	Rate, °C/hr.	7200	270			2300	2300
Lifetime, microseconds		10	14			14	10
Anneal:	Temperature, °C			450	450		
	Time, hours			5	20		
	Gas						
Quench:	High Temperature, °C			450	450		
	Final Temperature, °C			200	200		
	Rate, °C/hr.			167	167		
Lifetime, microseconds				21	21		

V. NEW TECHNOLOGY

Developments in this program which may be categorized as reportable under "New Technology" are summarized below:

1. P-On-N Lithium Diffused Silicon Solar Cell (as a new or improved device). Based on the findings of NAS5-9131 (RCA, Princeton) and related programs, a p-on-n silicon solar cell containing approximately 10^{17} lithium atoms per cc in the base region was developed. Cell voltage-current performance was comparable to conventional n-on-p and p-on-n silicon solar cells, with the best efficiency being 11%, air mass one. The resistance of this type of cell to high energy irradiation has been found markedly superior to any similar type of cell heretofore developed. Processing methods and device characteristics are reviewed in Section II -B of this report.

2. N-On-P Lithium Diffused Silicon Solar Cell (as a new or improved device). Based on the findings of NAS5-9131 (RCA, Princeton) and related programs, an n-on-p silicon solar cell containing 10^{15} to 10^{16} lithium atoms per cc in the base region was developed for the purpose of evaluating the interaction of lithium with radiation damage centers. The cell efficiency and radiation performance is comparable to conventional n-on-p cells. Processing methods and device characteristics are reported in Section II -A of this report.

3. Aluminum Antimonide P-On-N Solar Cell (as an improved device). 1 x 2 cm cells have been prepared by diffusing zinc or cadmium into n-type aluminum antimonide. State-of-the-art cells have conversion efficiencies below 3%. Deterioration of the cell performance is evident when exposed to air for prolonged periods of time. The contact materials are ultrasonically soldered lead(n-type) and silver (p-type). Cell processing and characteristics are presented in Section III of this report.

4. Boron Nitride Diffusant Source (as new application of older technology). Boron nitride had been used as a diffusant source in the processing of transistors prior to its utilization for solar cells. This program constitutes its first known use for solar cells, specifically whereby junctions 0.5 to 0.7 microns are formed. The boron nitride surface is etched with HF: 3 H_2O prior to diffusion. For solar cell applications, diffusion at 975°C. 25 minutes, gives approximately the same sheet resistance (55 to 65 ohms per square) and junction depths obtained using the more convetional phosphorus diffusions of 25 minutes, 875°C.

5. Lithium Nitride as Diffusant Source (as new technology). Powdered lithium nitride has been used successfully as a source for diffusing lithium into silicon. The results are illustrated in Figure 33 giving the bulk resistivity achieved for 30 and 50 minute diffusions into 1.5 ohm cm n-type float-zone silicon. About 50°C higher temperatures are required using lithium nitride than the lithium-oil suspension to achieve the same concentrations in the bulk silicon.

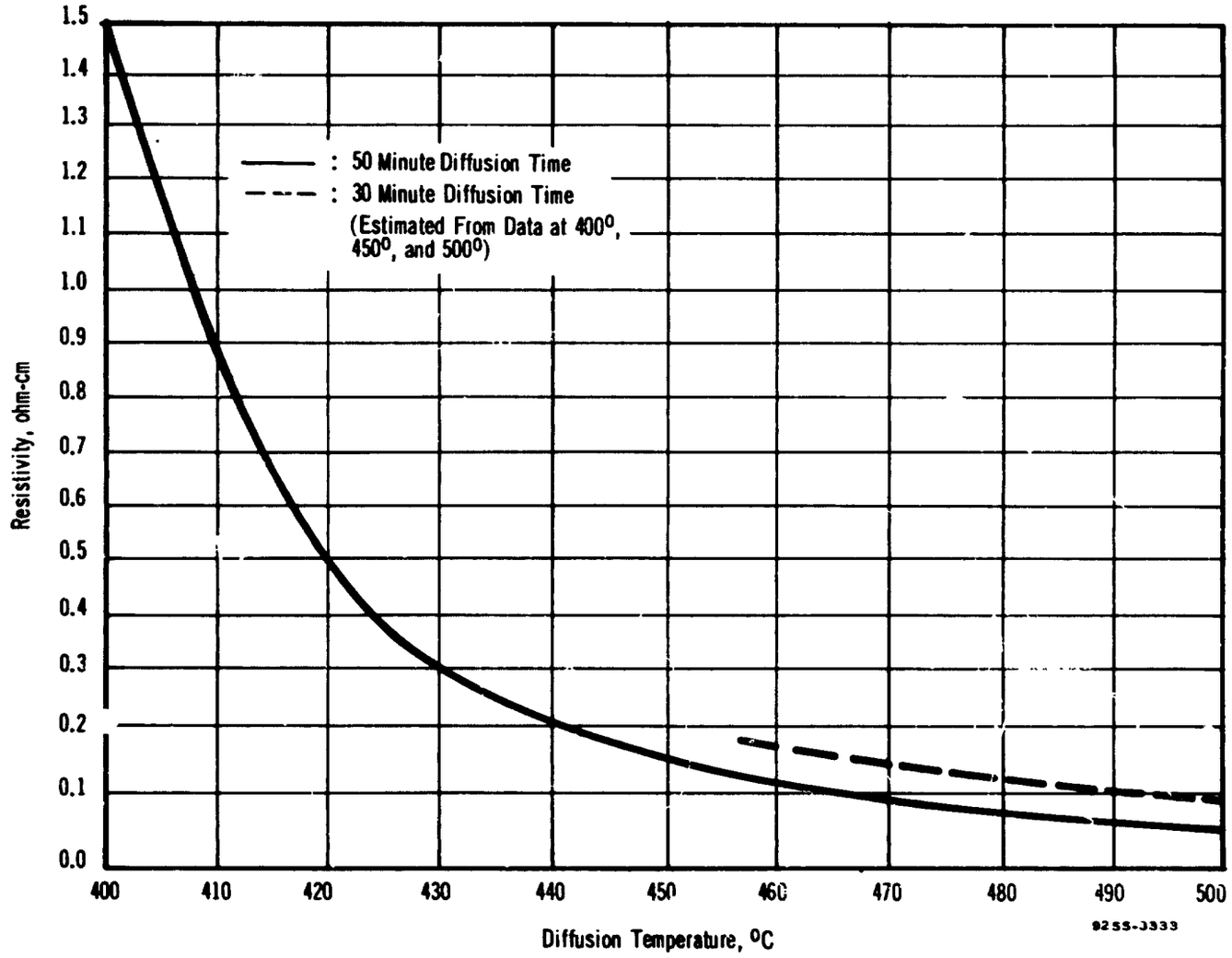

FIGURE 35. LITHIUM NITRIDE AS A DIFFUSANT SOURCE FOR SILICON SOLAR CELLS

VI. CONCLUSIONS

The p-on-n lithium diffused silicon solar cell is a major break-through in the search for a radiation resistant energy conversion device. Highly efficient cells can be made from either p- or n-type silicon of a very broad range of resistivities. However, the differences in radiation resistance of cells having these variables require further evaluation. Also, there are numerous anticipated interactions between the lithium and other material properties as dislocations and oxygen content. These reactions require evaluation specifically in solar cell structure and for environments to which it will be expcsed.

The application of aluminum antimonide as a solar cell base material of near optimum energy gap is as yet in a preliminary phase of development. The major problem is to keep the junction within the depth restrictions of about 1 micron as imposed by the short diffusion lengths of optically generated carriers. While the requirements of a suitable junction have not been found technically feasible using zinc or cadmium, modifications of the conventional diffusion methods may resolve this problem.

REFERENCES

1. N. Almeleh, B. Goldstein, J. J. Wysocki, and P. Rappaport, NASA Contract Report "Radiation Damage in Silicon," Final Report, Dec., 1964, Contract NAS5-3788 by RCA Laboratories, Princeton, New Jersey, prepared for NASA, Goddard Space Flight Center.

2. B. Goldstein, N. Almeleh, J. J. Wysocki, and P. Rappaport, NASA Contract Report "Analysis of Radiation Damage in Silicon Solar Cells and Annealing or Compensation of Damage by Impurities," July 1965, Contract NAS5-9131, RCA Laboratories, Princeton, New Jersey, for NASA, Goddard Space Flight Center.

3. N. B. Hannay, Semiconductors, Reinhold Publishing Co., page 217 (1960).

4. 1965 (RCA) Applied Research Project No. 262, "Effects of Selected Impurities on Solar Cells, Lithium Doped N-on-P Silicon Solar Cells," prepared by A. R. Topfer, Quarterly Report for period February 1965 to June 1965, RCA Special Electronic Components and Devices, Mountaintop, Pa., June 3, 1965.

5. R. Slang and W. B. Easton, J. Elec. Soc., Vol. 107, page 758 (1960).

6. O. N. Tufte, J. Elec. Soc., Vol. 109, page 235 (1962).

7. Boltaks, Diffusion in Semiconductors, Academic Press, N. Y., 1963.

8. "Materials Development for Solar Cell Applications," Second Quarterly Report, Contract NAS5-9576, prepared by A. R. Topfer, Electronic Components and Devices, RCA, Mountaintop, Pa., for NASA, Goddard Space Flight Center, Greenbelt, Md., December 14, 1965.

9. "Research on Materials Exhibiting Photovoltaic Phenomena," Technical Documentary Report ASD-TDR-62-841, Electro-Optical Systems, Jan. 1963.

10. "Materials Development for Solar Cell Applications," First Quarterly Report, Contract NAS5-9576, prepared by A. R. Topfer, Electronic Components and Devices, RCA, Mountaintop, Pa., for NASA, Goddard Space Flight Center, Greenbelt, Md., Oct. 4, 1965.

REFERENCES (Continued)

11. "Manufacturing Methods Program for Gallium Arsenide Solar Cells," Final Report, Technical Documentary Report No. ML-TDR-64-165, prepared under Contract No. AF33(657)-8921 by the Radio Corporation of America, Electronic Components and Devices, Somerville, New Jersey, prepared by R. Gold, et al, for A. F. Materials Laboratory, Wright-Patterson Air Force Base, Ohio, July 1964.

12. "Radiation-Resistant Silicon Solar Cells of Improved Efficiency," Final Technical Report, Contract No. NAS5-457, prepared by J. A. Baicker, et al, David Sarnoff Research Center, Princeton, New Jersey, for NASA, Goddard Space Flight Center, Greenbelt, Maryland, Dec. 15, 1963.